

## Accepted Manuscript

Research paper

Synthesis, crystal structure, electrochemical behavior and docking molecular of poly-nuclear metal complexes of Schiff base ligand derived from 2-amino benzyl alcohol

Pardis Roozbahani, Mehdi Salehi, Rahime Eshaghi Malekshah, Maciej Kubicki

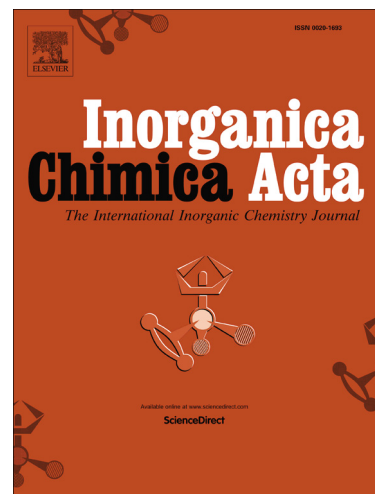
PII: S0020-1693(19)30601-2  
DOI: <https://doi.org/10.1016/j.ica.2019.119022>  
Article Number: 119022  
Reference: ICA 119022

To appear in: *Inorganica Chimica Acta*

Received Date: 1 May 2019  
Revised Date: 12 July 2019  
Accepted Date: 12 July 2019

Please cite this article as: P. Roozbahani, M. Salehi, R. Eshaghi Malekshah, M. Kubicki, Synthesis, crystal structure, electrochemical behavior and docking molecular of poly-nuclear metal complexes of Schiff base ligand derived from 2-amino benzyl alcohol, *Inorganica Chimica Acta* (2019), doi: <https://doi.org/10.1016/j.ica.2019.119022>

This is a PDF file of an unedited manuscript that has been accepted for publication. As a service to our customers we are providing this early version of the manuscript. The manuscript will undergo copyediting, typesetting, and review of the resulting proof before it is published in its final form. Please note that during the production process errors may be discovered which could affect the content, and all legal disclaimers that apply to the journal pertain.



# Synthesis, crystal structure, electrochemical behavior and docking molecular of poly-nuclear metal complexes of Schiff base ligand derived from 2-amino benzyl alcohol

Pardis Roozbahani<sup>a</sup>, Mehdi Salehi<sup>a,\*</sup>, Rahime Eshaghi Malekshah<sup>a</sup>, Maciej Kubicki<sup>b</sup>

<sup>a</sup>Department of Chemistry, Semnan University, Semnan, Iran

<sup>b</sup>Faculty of Chemistry, Adam Mickiewicz University, Umultowska 89b, 61-614 Poznan, Poland

## Correspondence

Mehdi Salehi, Department of Chemistry, Semnan University, P.O. Box 35195-363, Semnan, Iran. Email: msalehi@semnan.ac.ir

## Abstract

In the present work, we synthesized three novel Cu(II) and Mn(II) complexes (**1-3**) of a tridentate Schiff base ligand (H<sub>2</sub>L<sup>1</sup>) derived from 2-hydroxy-4-methoxybenzaldehyde and 2-amino benzyl alcohol. The Schiff base ligand and its complexes were characterized by FT-IR, UV-Vis and elemental analysis. The molecular structures of products were determined by X-ray diffraction, which confirmed the formation of bi-nuclear (**1**), tetra-nuclear (**2**) and tri-nuclear (**3**) complexes. In addition, the electrochemical properties of the complexes were examined by means of cyclic voltammetry in tetrahydrofuran, which showed the irreversible processes. Molecular docking studies of the free Schiff base ligand and its complexes were performed with BDNA and Interleukin-6 (PDB ID: 1BNA and 1alu). The results of docked models showed that ligand and complexes **1-3** preferentially bind to the minor groove of DNA receptor. In addition, complexes **1-3** exhibit higher binding affinity to Interleukin-6 as compared to ligand and drug of anticancer.

**Keywords:** Crystal structures, Di-, tetra and trinuclear complexes, Electrochemical behavior, Molecular docking, Interleukin-6.

## 1. Introduction

Much energy has been spent on the synthesis of tridentate Schiff base ligands and their complexes [1-3], owing to their high efficiency and stability. Therefore, these complexes have been studied for different applications as anti-bacterial, anti-virus, anti-cancer agents, in medical, and chemical industries, and so forth. Schiff bases derived from salicylaldehyde and their metal complexes play major roles in a wide range of fields [4-8]. Pahonțu et al. studied the antimicrobial activity of 2-hydroxy-4-methoxybenzaldehyde with ethyl-4-aminobenzoate and their six new Cu(II) complexes, showing that the antimicrobial effects of copper complexes are higher than those of ligands [9]. In another study, 4-substituted benzaldehyde derivatives were proved capable of preventing the synthesis of melanin in various dermatological disorders [10]. Matusiak et al. have shown that mono- and poly-nuclear copper complexes show effective phenoloxidase activity and cause apoptosis in vivo [11]. Jitaru and collaborators reported the antiferromagnetic properties of poly-nuclear Mn-oxo complexes Fe(III) and Mn(II, III) [12]. Also, Hureau revealed the synthesis of Mn(II) complex by the formation of mixed-valent di- $\mu$ -oxo-bridged dinuclear complexes  $[(L)Mn^{III}(\mu-O)_2Mn^{IV}(L)](ClO_4)_3$  [13]. Nowadays, millions of people suffer from cancer, as it is one of the most fatal diseases. Many platinum-based drugs such as cisplatin, carboplatin and oxaliplatin alone or in combination with other drugs are important chemotherapeutic agents inhibiting tumor growth in cancer therapy. Their use is more often than not accompanied by significant toxic side effects such as nephrotoxicity, drug resistance, renal and cervical problems, and they are often sensitive to resistance mechanisms [14, 15]. Therefore, there is an urgent need for more efficient anticancer drugs of non-platinum

complexes with significant anti-tumour activity and lower side effects compared to cisplatin. The discovery and development of new anti-cancers drugs is a long-term, time consuming and expensive process. Computer-aided drug discovery/design methods can act as a virtual shortcut in the pharmaceutical industry and academia; they reduce the number of ligands and are potentially less time consuming compared to the experimental procedures. Today, CADD has become an effective and indispensable tool in the discovery and design of pharmaceutical products [16]. In the current research, we introduced a simple procedure for the preparation of a new Schiff base ligand  $H_2L^1$  and its chelates with transition metal ions such as Cu(II) and Mn(II) (Schema 1). The  $H_2L^1$  ligand and its complexes were synthesized and studied by elemental analysis, IR, UV-Vis, and electrochemical behavior. Complexes **1 - 3** were characterized by X-ray crystallography, and molecular docking studies were discussed to elucidate the binding modes associated with the anti-cancer properties of compounds with DNA and Interleukin-6.

### Scheme 1.

#### 2.1. Materials and physical measurements

The solvents for synthesis were purchased from Merck and used without further purification. Elemental analysis was done on Elementar Vario EL III CHNOS Elemental Analyzer. FTIR spectra were obtained using a FT-IR SHIMADZU spectrophotometer and electronic spectra were carried out a Shimadzu UV-1650PC spectrophotometer. Electrochemical experiments were accomplished on a Metrohm 757VA Computrace instrument at room temperature in THF solution.

#### 2.2. Synthesis

##### 2.2.1. Synthesis of Schiff base ligand $H_2L^1$

The ligand was obtained from 2-hydroxy-4-methoxybenzaldehyde (1mmol, 0.152 g) and 2-amino benzyl alcohol (1mmol, 0.123 g). For preparation of this ligand, methanol was used as solvent. The mixture was stirred at room temperature for 3h. The resulting yellow precipitate collected through filtration and dried. Yield: 90%. Mol. Wt: 257.11 g/mol Anal. Calc. for  $C_{15}H_{15}NO_3$ : C, 70.02; H, 5.88; N, 5.44%; Found: C, 70.08; H, 5.87; N, 5.53%. FT-IR:  $\nu_{\max}$   $cm^{-1}$  (KBr): 3326, 3133, 2835, 1624, 1584, 1564, 1538, 1507, 1482, 1457, 1406, 1356, 1315, 1290, 1250, 1214, 1184, 1128, 1047, 1016, 966, 885, 839, 799, 759, 743, 708, 673, 601, 586, 525, 505, 465, 414. UV-Vis:  $\lambda_{\max}$  (nm) ( $CH_3CN$ ): 293, 417.

### 2.2.2. Synthesis of $Cu_2L_2$ and $Cu_4(L_4)$ (1 and 2)

Solution of  $Cu(OAc)_2 \cdot H_2O$  (0.5mmol, 0.09 g) in methanol was added to ligand (0.5 mmol, 0.128 g) and refluxed for 3 hours. The solution was filtered and two different kinds of crystals suitable for x-ray diffraction were selected from the solution after a week.

#### In Complex 1:

Yield: 75%. Mol. Wt: 637.61 g/mol. Anal. Calc. for  $C_{30}H_{26}Cu_2N_2O_6$ : C, 56.51; H, 4.11; N, 4.39%; Found: C, 56.28; H, 4.21; N, 4.35%. FT-IR:  $\nu_{\max}$   $cm^{-1}$  (KBr): 3167, 3128, 2930, 2852, 1736, 1686, 1653, 1608, 1576, 1565, 1516, 1488, 1455, 1400, 1323, 1279, 1241, 1202, 1175, 1124, 1086, 1031, 982, 833, 756, 657, 619, 553, 525, 481, 421. UV-Vis:  $\lambda_{\max}$  (nm) (THF): 277, 295, 335, 390, 602.

#### In Complex 2:

Yield 75%. Mol. Wt: 1421.40 g/mol. Anal. Calc. for  $C_{66}H_{66}Cu_4N_6O_{14}$ : C, 58.06; H, 6.26; N, 3.98%; Found: C, 58.02; H, 6.19; N, 3.94%. FT-IR:  $\nu_{\max}$   $cm^{-1}$  (KBr): 2959, 2939, 2845, 1617, 1538, 1493, 1467, 1445, 1429, 1396, 1362, 1318, 1220, 1175, 1124, 1070, 1031, 976, 932, 910,

849, 799, 744, 650, 589, 567, 506, 463, 429, 407. UV–Vis:  $\lambda_{\max}$  (nm) (THF): 260, 263, 308, 388, 592.

### 2.2.2. Synthesis of $\text{Mn}_3\text{L}^1_2\text{L}^2_2(\text{OAc})_2 \cdot \text{EtOH}$ (**3**)

The novel complex **3** was synthesized according to the procedure similar to one mentioned above for complex **1**. The solution was dried and recrystallized in an acetonitrile:ethyl acetate 1:1 mixture. Crystals suitable for x-ray crystallography were obtained after two weeks. Yield: 73%. Mol. Wt: 1141.77 g/mol Anal. Calc. for  $\text{C}_{50}\text{H}_{46}\text{Mn}_3\text{N}_2\text{O}_{16} \cdot \text{C}_2\text{H}_5\text{OH}$ : C, 57.10; H, 4.79; N, 2.66; Found: C, 56.28; H, 4.69; N, 2.80%. FT-IR:  $\nu_{\max}$   $\text{cm}^{-1}$  (KBr): 1612, 1584, 1557, 1528, 1497, 1406, 1370, 1304, 1212, 1186, 1124, 1018, 977, 850, 799, 764, 667, 621, 534, 412. UV–Vis:  $\lambda_{\max}$  (nm) (THF): 206, 273, 390.

### 2.3. X-ray crystallography

Diffraction data was collected by the  $\omega$ -scan technique at 130(1) K (**1**) and at 100(1) K (**2**, **3**) on Rigaku XCalibur four-circle diffractometer with EOS CCD detector and graphite-monochromated  $\text{MoK}_\alpha$  radiation ( $\lambda=0.71073$  Å). The data was corrected for Lorentz-polarization as well as for absorption effects [17]. Precise unit-cell parameters were determined by a least-squares fit of 3943 (**1**), 9173 (**2**) and 7908 (**3**) reflections of the highest intensity, chosen from the whole experiment. The structures were solved with SHELXT-2013 [18] and refined with the full-matrix least-squares procedure on  $F^2$  by SHELXL-2013 [18]. All non-hydrogen atoms were refined anisotropically, hydrogen atoms were placed in idealized positions and refined as ‘riding model’ with isotropic displacement parameters set at 1.2 (1.5 for methyl and hydroxyl groups) times  $U_{\text{eq}}$  of appropriate carrier atoms. In the structure **3** the C-C distance in the solvent (ethanol) molecule was restrained to typical value (DFIX).

Crystallographic data for the structural analysis was deposited with the Cambridge Crystallographic Data Centre, Nos. CCDC-1855697 (**1**), CCDC-1885977 (**2**) and CCDC-1855698 (**3**). The Copies of this information may be obtained free of charge from: The Director, CCDC, 12 Union Road, Cambridge, CB2 1EZ, UK; e-mail: [deposit@ccdc.cam.ac.uk](mailto:deposit@ccdc.cam.ac.uk), or [www.ccdc.cam.ac.uk](http://www.ccdc.cam.ac.uk).

#### **2.4. Electrochemical studies**

The electrochemical experiments of the synthesized complexes **1-3** were performed by means of cyclic voltammetry with 0.1 mol/dm<sup>3</sup> tetrabutylammonium hexafluorophosphate (TBAH) as supporting electrolyte and complexes concentration of about 1×10<sup>-3</sup> mol/dm<sup>3</sup> in THF. All electrode potentials were calibrated using the redox potential of the ferrocene/ferrocenium couple as reference. The three-electrode cells were comprised of auxiliary platinum, a reference Ag wire and glassy carbon as the working electrode. The solutions were deoxygenated by purging dry Argon through the solution for 5 min prior to each experiment.

#### **2.5. Molecular docking of the compounds with DNA duplex of sequence (PDB ID: 1BNA) and Interleukins (PDB ID: 1alu)**

To fathom the antitumor activity and the binding site of the target-specific region of compounds, we used molecular docking simulation. The crystal structures of 1BNA (B-DNA Dodecamer: right-handed double-stranded B helix (as rigid molecule) with the sequence (5'-D(CpGpCpGpApApTpTpCpGpCpG)-3'), Interleukins (PDB ID: 1alu, (as rigid molecule)) and anticancer drugs were downloaded from RCSB Protein Data Bank ([ww.rcsb.org/pdb](http://www.rcsb.org/pdb)) and Pubchem. The ligand H<sub>2</sub>L<sup>1</sup> (as flexible ligand) was optimized via standard 6-31G\*\* basis sets. Complexes **1**, **2** and **3** (as flexible ligand) were taken from the crystal structures as a CIF file and converted to the PDB format using Mercury software. The molecular docking simulation and

calculations were performed by AutoDock 4.2 (The Scripps Research Institute, La Jolla, CA, USA) with AutoGrid 4 and AutoDock 42, meaning all non-ring torsions were maintained. Primarily, the heteroatoms including water molecules around the duplex were removed using AutoDock tools; polar hydrogen atoms, Kollman united atom type charges and Gasteiger partial charges were then added to the receptor molecule. All the docking simulations were defined by use of a grid box with  $74 \times 64 \times 117$  Å points with a grid-point spacing of 0.375 Å for BNA, a grid box with a size of  $126 \times 126 \times 126$  Å with a grid-point spacing of 0.375 Å for IL-6. To study this interaction, the molecular docking using a Lamarckian genetic algorithm method was engaged. The number of genetic algorithm runs and the number of evaluations were set to 100. The most optimized model with the lowest energy was selected from the one minimum energy (root mean square deviation, RMSD = 0.0) and 100 runs to compare the structural similarity. After that, the interactions of BNA and Interleukin and their binding modes with compounds were analyzed using AutoDock program, UCSF Chimera 1.5.1 software, Discovery Studio 3.0 from Accelrys and DS Visualizer.

### **3. Results and discussion**

#### **3.1. Synthesis**

The novel Schiff base ligand was synthesized by reacting 2-hydroxy-4-methoxybenzaldehyde with 2-amino benzyl alcohol in methanol. Complexes **1-3** were synthesized by reacting  $\text{Cu}(\text{CH}_3\text{CO}_2)_2 \cdot \text{H}_2\text{O}$  or  $\text{Mn}(\text{CH}_3\text{CO}_2)_2 \cdot 4\text{H}_2\text{O}$  with Schiff base ligand in methanol.  $\text{H}_2\text{L}^1$  ligand was soluble in common organic solvents like methanol, ethanol, acetonitrile and dichloromethane, but complexes **1-3** were readily soluble in THF. These compounds were characterized by elemental analysis, FT-IR, UV-Vis and Cyclic Voltammetry (CV) methods. Furthermore, complexes **1-3** were structurally characterized by X-ray crystallography.

### 3.2. Infrared spectra of ligand and its complexes

The structure can be easily verified through comparing the IR spectra of the free ligand with those of their metal complexes (Figs. S<sub>1</sub>, S<sub>3</sub>, S<sub>5</sub> and S<sub>7</sub>). The  $\nu(\text{C}=\text{N})$  absorption band of the ligand at  $1624\text{ cm}^{-1}$  was shifted towards lower energies  $1608$ ,  $1617$  and  $1612\text{ cm}^{-1}$  in the spectra of complexes **1**, **2** and **3**, respectively, suggesting the back bonding from the metals to the orbital of azomethine nitrogen [19]. The phenolic  $\nu(\text{C}-\text{O})$  stretching vibration of the free Schiff base ligand was observed at  $1128\text{ cm}^{-1}$ , and was shifted towards lower wave numbers after complexation for complexes **1**, **2** and **3** to  $1086$ ,  $1070$  and  $1124\text{ cm}^{-1}$ , respectively, suggesting the participation of phenolic oxygen atoms linked to the  $\text{Cu}^{2+}$  and  $\text{Mn}^{2+}$  ions [20]. The signals  $1565$  and  $1400\text{ cm}^{-1}$  in complex **1** can be assigned to the bonding of  $\nu_{\text{asym}}(\text{C}-\text{O}-\text{Cu})$  (bidentate) and  $\nu_{\text{sym}}(\text{C}-\text{O}-\text{Cu})$  (bidentate), respectively. In addition, the intense bands at  $1538$  and  $1396\text{ cm}^{-1}$  were assigned to  $\nu_{\text{asym}}(\text{C}-\text{O}-\text{Cu})$  (bidentate) and  $\nu_{\text{sym}}(\text{C}-\text{O}-\text{Cu})$  (bidentate vibrations), respectively in complex **2**. These results show that the acetate group acted as a bidentate bridging ligand. Furthermore, the absorptions appearing at  $1557$  and  $1406\text{ cm}^{-1}$  for complex **3** indicated the asymmetric and symmetric stretching frequencies of the acetate ( $\mu\text{-RCO}_2$ ) groups, respectively [12, 21]. The broad band exhibited at  $3000\text{--}3500\text{ cm}^{-1}$  in the spectra of the free ligand is due to the stretching vibration of  $\nu_{\text{OH}}$ . The new bands appearing at  $553\text{--}421$ ,  $567\text{--}429$  and  $621\text{--}412\text{ cm}^{-1}$  for complexes **1**, **2** and **3**, respectively, were assigned to  $\nu(\text{M}-\text{O})$  and  $\nu(\text{M}\leftarrow\text{N})$  vibrations, respectively [22].

### 3.3. UV spectra of compounds

UV-Vis spectra for ligand and its complexes were reported at a wavelength range of  $200\text{--}800\text{ nm}$  (Figs. S<sub>2</sub>, S<sub>4</sub>, S<sub>6</sub> and S<sub>8</sub>). UV-Vis spectrum of ligand did not have any absorption peak of d-d transition, but it exhibited maximum absorption bands around  $293$  and  $417\text{ nm}$  associated with n-

$\pi^*$  and  $\pi-\pi^*$  transitions, respectively [23, 24]. One band was observed in regions 277, 260 and 206 regarding complexes **1-3**, respectively, which are assignable to LC transitions of the aromatic groups [25]. The absorption bands of complex **1** and **2** at 335-390 and 388 nm were specified to  $n-\pi^*$  transition, and the absorption bands around 295 and 308 nm were due to  $\pi-\pi^*$  transition in complexes **1** and **2**, respectively. Complexes **1** and **2** exhibited only one broad d-d band, centered in the region of 602 and 592 nm [26, 27]. The band at 273 nm in **3** is related to  $\pi-\pi^*$  transition, while the peak around 390 nm belongs to ligand-metal charge transfer transitions  $n\rightarrow\pi^*$ . It is to be noted that no d-d transition was expected for complex **3** [28-30].

### 3.4. Description of Crystal Structures

Figures 1-5 show the perspective view of the molecules. The collected data and refinement parameters are summarized in Table 1. Table 2 lists the relevant geometrical parameters. Binuclear  $\text{Cu}_2\text{L}^1_2$  complex **1** is  $C_i$ -symmetrical, as it lies across the inversion center (space group  $P2_1/n$ ), hence the fact that  $\text{Cu}_2\text{O}_2$  ring is planar. Cu ions are 4-coordinated in a quite regular square-planar environment – the four coordination centers make an, approximate plane (maximum deviation from the least-squares plane is 0.052(1)Å), and the Cu ion lies well within this plane (deviation 0.028(1)Å). Four-nuclear  $\text{Cu}_4(\text{L}^1_4)$  complex **2** is also  $C_i$ -symmetrical, as it lies across the inversion center (space group  $P-1$ ). Cu ions are 5-coordinated in a quite regular square-pyramidal environment. In tri-nuclear  $\text{Mn}_3\text{L}^1_2\text{L}^2_2(\text{CH}_3\text{COO})_2$  complex **3**, all three Mn centers are six-coordinated in an octahedral fashion. The neighboring cations are bridged by O atoms from acetate fragments of both ligand molecules; terminal Mn ions are additionally coordinated by NO centers from  $\text{L}^1$  molecules. Hence, terminal metal ions are  $\text{NO}_5$  coordinated, while the central cation is  $\text{O}_6$ -coordinated. Figure 4 shows the details of coordination scheme. The conformation of ligand  $\text{L}^1$  molecules, as defined by dihedral angles between planar

fragments, depends on the complex (cf. Figure. 5, Table 2): this molecule is more planar in **1**, while it is significantly twisted in the more sterically demanding complex **2**.

In crystal structures, electrostatic and dispersive interactions are mainly responsible for the crystal architectures. In **2**, the solvent-ethanol molecules are hydrogen-bonded with the complex (one of the acetates: H $\cdots$ O 2.13Å, O $\cdots$ O 2.920(7)Å, O-H $\cdots$ O 157°).

**Tables 1-2.**

**Fig.s 1-5.**

### 3.5. Electrochemistry

The electrochemical properties of metal complexes were studied in order to explain minor spectral and structural changes accompanying electron transfer. The compounds were homogenized by magnetic stirring with THF and the voltammograms are shown in Figures 6-8. The cyclic voltammograms of **1** and **2** showed one cathodic peak potential (E<sub>pc</sub>) Cu<sup>(II)</sup>/Cu<sup>(I)</sup> at -0.91 and -1.07 V, respectively. In the anodic peaks of complex **1**, the two direct oxidation of Cu(I)  $\rightarrow$  Cu(II) were observed at E<sub>pa</sub> = 0.826 and 1.17 V. Meanwhile, in complex **2**, the two direct oxidation of Cu(I)  $\rightarrow$  Cu(II) were observed at E<sub>pa</sub> = 0.3, 0.47 V and one direct oxidation of Cu(0)  $\rightarrow$  Cu(I) was observed at E<sub>pa</sub> = 1.33 V. Complexes **1** and **2** displayed an irreversible oxidation wave [4, 31]. Complex **3** is electroactive with respect to the metal center and exhibits two redox processes associated with a two-electron transfer at room temperature. Under identical experimental conditions, the cathodic potentials (E<sub>pc</sub>) values for **3** were -0.76 (Mn<sup>III</sup>/Mn<sup>II</sup>) and 1.64 V (Mn<sup>II</sup>/Mn<sup>I</sup>), and the corresponding E<sub>pa</sub> (Mn<sup>II</sup>/Mn<sup>III</sup>) value was 0.195. As shown in Figure 8, complex **3** exhibited irreversible characteristic [13, 32].

**Fig.s 6-8.**

### 3.6. Molecular docking compounds with BNA

Cancer is one of the most fatal diseases, originating from different cancer-causing agents (carcinogens) ranging from environmental pollutants to genetic mutations [33]. DNA is the primary intracellular target of anticancer drugs that intercalate into DNA and interfere with the activity of topoisomerases when they bind to nuclear DNA. Over the recent decades, DNA-binding molecules have become critically important in clinical cancer therapy [34]. Generally, many antitumor drugs have shown their cytotoxic effect on replication, transcription and consequent induction of programmed cell death (PCD [35-37]. In areas of pharmaceutical research, it is necessary to discover and synthesize possible effective DNA–metal complexes as chemotherapeutic agents and the interaction modes and mechanism of such compounds. Binding affinity of the compounds and the hydrogen bonding interactions with DNA estimated at the molecular level is based on physical interactions (electrostatic, van der Waals, hydrophobic, specific hydrogen bonding, etc.). One of the extensively developing trends in computer simulations is the prediction of pharmacological action of drugs at the molecular level and a strong base for the experimental synthesis of novel bioactive molecules. Molecular docking simulation is one of the most valuable approaches to predicting the interaction of all possible configurations and determining the optimal orientation of compounds between biological macromolecule-compounds [37, 38]. The lowest energy conformations were rated based on docking calculations of the lowest free binding energy. The docking results are shown as binding free energy in Figure. 9 and listed in Table 3. The minimum energy of each compound was applied to the best possible geometry of compounds inside the DNA double helix. Moreover, anti-cancer chemotherapeutic drugs, Mitoxantrone and Trifluridine (FTD) as DNA-drug interaction, were used to compare their results with the compounds. The calculated binding free

energies ( $\Delta G_{\text{binding}}$ ) for the free ligand, complexes **1**, **2**, **3** and anti-cancer drugs to DNA (Trifluridine and Mitoxantrone) were -7.56, -7.74, -6.45, -9.87, -9.09 and -5.88 kcal/mol, respectively; the binding of the compounds to the DNA is spontaneous. The more negative relative binding energy of complex **3** suggests more ability to bind to the DNA compared with the free ligand and complexes **1**, **2** and anti-cancer drugs to DNA (Trifluridine and Mitoxantrone) [39, 40]. Results suggest that complex **3** can act as the DNA-damaging anticancer agent. Moreover, the binding free energy values were dominated by the vdW + Hbond + desolv energy (kcal/mol) energy in the final energy, which is principally related to the formation of hydrogen bonds between the compounds and receptor. The lowest-energy conformations show that all the compounds bind to the minor groove. In order to determine the binding site and to obtain information about the hydrogen bonding interactions of the compounds, hydrogen bonding interactions are illustrated in Figure. 10. As shown in Figure. 10, there are two hydrogen bonding interactions between OH of the ligand and the phosphate oxygen atoms of DNA helix 2.06 and 2.28 (Å), respectively. On the other hand, complexes **1** and **3** interacted with DNA through hydrogen bonding with DC116 (2.96 Å) and DA55 (1.71 Å), respectively. However, complex **2** interacted with phosphates and ribose group through hydrogen bonding 2.85 and 2.98 Å, respectively [40]. Moreover, Trifluridine interacted with groups of guanine DG110 (2.54 Å) and DG116 (1.69 Å) by forming hydrogen bonds, meanwhile, Mitoxantrone displayed hydrogen bond interaction with DA118 (1.89 Å).

**Fig.s 9-10.**

**Table 3.**

### **3.7. Molecular docking of compounds with Interleukin 6**

The increase in the levels of IL-6 augments the tumor growth risk, and weakens the immune systems of HIV-positive people. Human interleukin-6 (IL6) is one such inflammatory molecule,

produced and secreted by tumor cells into IL-6 receptor  $\alpha$ (IL-6R $\alpha$ ) subunit of microenvironment [41]. It is involved in the proliferation, survival, and metastatic dissemination of malignant cells, and it is abundantly found in the serum and tumor tissues of a majority of cancers, namely gastric, multiple myeloma, melanoma, pancreatic, breast, colorectal, myeloma, cervical and lung cancer. A lower level of IL-6 is associated with a better response to therapy. Anticancer drugs and ionizing radiation used during cancer therapy induce the expression of different pro-inflammatory cytokines (IL-6), chemokines and anti-apoptotic genes in tumor by activating STAT-3 and NF- $\kappa$ B signaling, which leads to the resistance of cells to chemotherapy. Moreover, IL-6, a potent immunosuppressive cytokine, plays an important role in protecting cancer cells from therapy-induced DNA damage, oxidative stress, endogenous and exogenous (chemotherapy drugs, ionizing radiation) damage and apoptosis [42, 43]. These observations suggest that IL-6 is blocked for therapy in cancers. The present study was conducted to design and develop the exploration of IL-6 inhibitors with high efficiency and high selectivity based on molecular docking calculations. The docking calculations of compounds were further performed to describe the mode of binding to Interleukin-6. The values of docking energy were -5.71, -7.66, -7.72, -7.70 and -6.34 kcal/mol for ligand, **1**, **2**, **3** and Lenalidomide, respectively, Fig. 11, Table 4. Comparing the relative binding energy ( $\Delta G_{\text{binding}}$ ) of compounds with Interleukin-6 proved that complex **2** was more effective than other compounds and the anti-cancer drug (Lenalidomide). The active sites of compounds and drug are shown in Fig 11. The interaction between the ligand and Interleukin-6 were dominated by hydrogen bonds Ser A175 and Glu A172 in site Helix D. No H-bonds were observed for complex **1**, but complex **1** was docked into the active site II. In addition, a hydrogen interaction is suggested between Lys A128 residue in the active site II and O-CH<sub>3</sub> of aromatic ring for complex **2**. Finally, complex **3** was able to interact with the Helix S

of Interleukin-6 by the hydrogen bond between O-CH<sub>3</sub> of aromatic ring and Lys A150. Complexes **1-3** proved to be potent anti-cancer agents compared with ligand with DNA and Interleukin-6 in computer-aided molecular docking studies. In addition, the results of molecular docking showed that complex **2** is a potential therapeutic strategy for the development of new chemotherapeutic drugs regarding the treatment of cancers as IL-6 inhibitors.

**Table 4.**

**Fig 11.**

#### **4. Conclusion**

Metal complexes of the Schiff base were synthesized and characterized by use of elemental analyses, cyclic voltammetry (CV), electronic absorption and IR- spectroscopy. The crystal structures of all complexes were determined by X-ray crystallography. The X-ray structure determination showed that the structures around Cu(II) (**1** and **2**) and Mn(II) (**3**) were square-planar, square-pyramidal and octahedral geometry, respectively. The electrochemical reduction of these complexes in THF solution is electrochemically irreversible. The compounds were computationally investigated by use of molecular docking simulation. Our data points to the higher probability of the interaction in the minor groove of DNA helix. Based on the docking simulation, complexes were found to have stronger binding propensity as compared to ligand.

#### **Acknowledgements**

We thank Semnan University for supporting this study.

#### **References**

[1] M. Choudhary, R.N. Patel, S.P. Rawat, "Synthesis, electrochemical, structural, spectroscopic and biological activities of mixed ligand copper(II) complexes with 2-{{(Z)}-(5-bromo-2-

hydroxyphenyl)methylidene]amino} benzoic acid and nitrogenous bases”, *J. Mol. Struct.* 1060 (2014) 197–207.

[2] A. Sreekanth, M.R.P. Kurup, “Structural and spectral studies on four coordinate copper(II) complexes of 2-benzoylpyridine *N*(4), *N*(4)- (butane-1,4-diyl)thiosemicarbazone”, *Polyhedron*. 22 (2003) 3321-3332.

[3] R.N. Patel, S.P. Rawat, M. Choudhary, Vishnu P. Sondhiya, Dheerendra K. Patel, K.K. Shukla, Dinesh K. Patel, Y. Singh, R. Pandey, “Synthesis, structure and biological activities of mixed ligand copper(II) and nickel(II) complexes of *N'* -(1*E*)-[(5-bromo-2-hydroxyphenyl) methylidene]benzoylhydrazone”, *Inorg. Chim. Acta.* 392 (2012) 283–291

[4] M.Tyagi, S. Chandra, P. Tyagi, “Mn(II) and Cu(II) complexes of a bidentate Schiff’s base ligand: Spectral, thermal, molecular modelling and mycological studies”, *Spectrochim Acta A Mol Biomol Spectrosc.*, 117 (2014) 1-8.

[5] Q. Liu, Y. Yang, W. Hao, Zh. Xu, L. Zhu, “Synthesis, Characterization and Biological Activity of Cis- Dioxomolybdenum(VI) Schiff base Complex [MoO<sub>2</sub>(L)<sub>2</sub>] ”, *IERI Procedia*. 5 (2013) 178-183.

[6] T. Rosu, E. Pahontu, C. Maxim, R. Georgescu, N. Stanica, G. L. Almajan, A. Gulea, “Synthesis, characterization and antibacterial activity of some new complexes of Cu(II), Ni(II), VO(II), Mn(II) with Schiff base derived from 4-amino-2,3-dimethyl-1-phenyl-3-pyrazolin-5-one”, *Polyhedron* 29 (2010) 757–766.

[7] N. Charef, F. Sebti, L. Arrar, M. Djarmouni, N. Boussoualim, A. Baghiani, S. Khennouf, A. Ourari, M. A. AlDamen, M. S. Mubarak, D. G. Peters, “Synthesis, characterization, X-ray structures, and biological activity of some metal complexes of the Schiff base 2,20 - (((azanediylbis (propane-3,1-diyl)) bis(azanylylidene))bis(methanylylidene))diphenol”, *Polyhedron*. 85 (2015) 450–456.

[8] D.C. Iliesa, E. Pahontuc, S. Shovad, R. Georgescue, N. Stanicaf, R. Olara, A. Guleag, T. Rosu, “Synthesis, characterization, crystal structure and antimicrobial activity of copper(II) complexes with a thiosemicarbazone derived from 3-formyl-6- methylchromone”, *Polyhedron*, 15 (2014) 123-131.

[9] E. Pahonțu, D. C. Ilieș, S. Shova, C. Paraschivescu, M. Badea, A. Gulea, T. Roșu, “Synthesis, Characterization, Crystal Structure and Antimicrobial Activity of Copper(II) Complexes with the

Schiff Base Derived from 2-Hydroxy-4-Methoxybenzaldehyde”, *Molecules.*, 20 (2015) 5771-5792.

[10] W. Yi, R. Cao, W. Peng, H. Wen, Q. Yan, B. Zhou, L. Ma, H. Song, “Synthesis and biological evaluation of novel 4-hydroxybenzaldehyde derivatives as tyrosinase inhibitors”, *Eur. J. Med. Chem.* 45 (2010) 639–646.

[11] A. Matusiak, M. Kuczer, E. Czarniewska, G. Rosiński, T. Kowalik-Jankowska, “Copper(II) complexes of alloferon 1 with point mutations (H1A) and (H9A) stability structure and biological activity”, *J. Inorg. Biochem.* 138 (2014) 99–113.

[12] I. Jitaru, E.M. Ungureanu, M.G. Alexandru, “Synthesis and characterization of new Mn (II, III) and Fe(III) oxo polynuclear complexes”, *U.P.B. Sci. Bull., Series B*, 69 (2007) 11-20.

[13] Ch. Hureau, G. Blondin, M. F. Charlot, Ch. Philouze, M. Nierlich, M. Césarío, E. Anxolabéhère-Mallart, “Synthesis, Structure, and Characterization of New Mononuclear Mn(II) Complexes. Electrochemical Conversion into New Oxo-Bridged Mn<sub>2</sub>(III,IV) Complexes”. Role of Chloride Ions, *Inorg. Chem.* 44 (2005) 3669–3683.

[14] C. Karthick, K. Karthikeyan, Purna Sai Korrapati, A. Kalilur Rahiman, Antioxidant, “DNA interaction, molecular docking and cytotoxicity studies of aminoethylpiperazine-containing macrocyclic binuclear copper(II) complexes”, *Appl Organometal Chem* 2016; 1–15

[15] D. Ning, Y. Cao, Y. Zhang, L. Xia, G. Zhao, “Structures and antitumor activities of planar chiral cyclopalladated ferrocene derivatives”, *Inorg chem commun.*, 58 (2015) 57–59.

[16] Talambedu Usha, Dhivya Shanmugarajan, Arvind Kumar Goyal, Chinaga Suresh Kumar, Sushil Kumar Middha, Recent Updates on Computer-aided Drug Discovery: Time for a Paradigm Shift, *Curr Top Med Chem.*, 2017, 17, 3296-3307.

[17] Agilent Technologies, CrysAlis PRO (Version 1.171.33.36d), Agilent Technologies Ltd, 2011.

[18] G. M. Sheldrick, *Acta Crystallogr.*, 2015, **A71**, 3-8.

[19] M. Salehi, F. Ghasemi, M. Kubicki, A. Asadi, M. Behzad, M. H. Ghasemi, A. Gholizadeh, “Synthesis, characterization, structural study and antibacterial activity of the Schiff bases derived from sulfanilamides and related copper(II) complexes”, *Inorg. Chim. Acta.* 453 (2016) 238–246.

- [20] H. Karimi-Maleh, M. Salehi, F. Faghani, application of novel Ni(II) complex and ZrO<sub>2</sub> nanoparticle as mediators for electrocatalytic determination of N-acetylcysteine in drug samples”, *J Food Drug Anal.* 25 (2017) 1000-1007.
- [21] O. N. Shishilov, N. S. Akhmadullina, Y. N. Rezinkova, R. E. Podobedov, A. V. Churakov, I. A. Efimenko, “Reactivity of polynuclear palladium carboxylate complexes towards acetonitrile. Synthesis and X-ray study of Pd<sub>2</sub>(C<sub>6</sub>H<sub>4</sub>-O-C(=NH)CH<sub>3</sub>)<sub>2</sub>(CH<sub>3</sub>CO<sub>2</sub>) and Pd<sub>5</sub>(CH<sub>3</sub>C(=N)OC(=N)CH<sub>3</sub>)(NO)(NO<sub>2</sub>)<sub>x</sub>(RCO<sub>2</sub>)<sub>7-x</sub>”, *Dalton Trans.* 14 (2013) 3712-3720.
- [22] S.A. Abdel-Latifa, H.B. Hassib, Y.M. Issa, “Studies on some salicylaldehyde Schiff base derivatives and their complexes with Cr(III), Mn(II), Fe(III), Ni(II) and Cu(II)”, *Spectrochim. Acta Part A.* 67 (2007) 950–957.
- [23] L. H. Abdel-Rahman, A. M. Abu-Dief, R. M. El-Khatib, Sh. M. Abdel-Fatah, “Some new nano-sized Fe(II), Cd(II) and Zn(II) Schiff base complexes as precursor for metal oxides: Sonochemical synthesis, characterization, DNA interaction, in vitro antimicrobial and anticancer activities, *Bioorganic Chem.*”, 69 (2016) 140-152.
- [24] J. Renjitha, G. S. Thara, “Synthesis and spectral studies of zinc (II) complexes of a Schiff base derived from isatin hydrazone and 2-hydroxy naphthaldehyde”, *AIP Conference Proceedings* 1849, (2017) 020036; doi: 10.1063/1.4984183.
- [25] Z. Abbasi, M. Salehi, M. Kubicki, Ali Khaleghian, “New Ni(II) complexes involving symmetrical bidentate N,O-donor Schiff base ligands: synthesis at ambient temperature, crystal structures, electrochemical study, antioxidant and cytotoxic activities”, *J. Coord. Chem.* 70 (2017) 3132–3146
- [26] L. Kafi-Ahmadi, L. Shirmohammadzadeh, “Synthesis of Co(II) and Cr(III) salicylidenic Schiff base complexes derived from thiourea as precursors for nano-sized Co<sub>3</sub>O<sub>4</sub> and Cr<sub>2</sub>O<sub>3</sub> and their catalytic, antibacterial properties”, *J. Nanostruct Chem.*, (2017). 10.1007/s40097-017-0221-x
- [27] K. Kadiravansivasamy, S. Sivajiganesan, T. Periyathambi, V. Nandhakumar, S. Chidhambaram, R. Manimekalai, “Synthesis and Characterization of Schiff Base Co<sup>II</sup>, Ni<sup>II</sup> and Cu<sup>II</sup> Complexes Derived from 2-Hydroxy-1-naphthaldehyde and 2-Picolylamine”, *Mod Chem appl.*, 5 (2017). DOI: 10.4172/2329-6798.1000197

- [28] S. J Shivhare, R. Mishra, A. GHaria, "Synthesis, characterization and antimicrobial studies of Cu(II), Co(II) and Ni(II) complexes with Schiff base derived from N- amino rhodanine and salicylaldehyde", *J Mol Struct.* 702 (2004) 49-54.
- [29] H. Ünver, A. Karakas, A. Elmali, "Nonlinear optical properties, spectroscopic studies and structure of 2-hydroxy-3-methoxy-N-(2-chloro-benzyl)-benzaldehyde-imine", *J Mol Struct.* 702 (2004) 49-54.
- [30] R. C. Maury, P. Patel, S. Rajput, "Synthesis and Characterization of Mixed-Ligand Complexes of Cu(II), Ni(II), Co(II), Zn(II), Sm(III), and U(VI)O<sub>2</sub>, with a Schiff Base Derived from the Sulfa Drug Sulfamerazine and 2,2'-Bipyridin", *Coord Chem*, 33 (2003) 801-816.
- [31] B. Sarkar, G. Bocelli, A. Cantoni, A. Ghosh, "Copper(II) complexes of symmetrical and unsymmetrical tetradentate Schiff base ligands incorporating 1-benzoylacetone: Synthesis, crystal structures and electrochemical behavior", *Polyhedron*. 27 (2008) 693-700.
- [32] S. A. Patil, M. Manjunatha, A. D. Kulkarni, P. S. Badami, "Synthesis, characterization, fluorescence and biological studies of Mn(II), Fe(III) and Zn(II) complexes of Schiff bases derived from Isatin and 3-substituted-4-amino-5-mercapto-1,2,4-triazoles", *Complex Metals*. 1 (2014) 128-137.
- [33] A. Terenzi, L. Tomasello, A. Spinello, G. Bruno, C. Giordano, G. Barone, "(Dipyrido[3,2-a:2',3'-c]phenazine)(glycinato)copper(II) perchlorate: A novel DNA-intercalator with anti-proliferative activity against thyroid cancer cell lines", *J. Inorg. Biochem.*, 117 (2012) 103-110.
- [34] S. Tabassum, M. Zaki, M. Afzal, F. Arjmand, "Synthesis and characterization of Cu(II)-based anticancer chemotherapeutic agent targeting topoisomerase Ia: In vitro DNA binding, pBR322 cleavage, molecular docking studies and cytotoxicity against human cancer cell lines", *Eur J Med Chem.*, 74 (2014) 509-523.
- [35] R. E. Malekshah, M. Salehi, M. Kubicki, A. Khaleghian, "Biological studies and computational modeling of two new copper complexes derived from  $\beta$ -diketones and their nano-complexes", *J. Mol. Struct.*, 1150, 2019. <https://doi.org/10.1080/00958972.2019.1606422>
- [36] R. E. Malekshah, M. Salehi, M. Kubicki, A. Khaleghian, "Synthesis, Molecular Structures, Apoptosis-Inducing Activity and Cytotoxicity in Vitro of Two New Zn(II)

Complexes with 2- Thenoyltrifluoroacetone and *N*-Donor Heterocyclic Ligands, *J. Mol. Struct.*, 1150 (2017) 155–165.

[37] R. Eshaghi Malekshah, M. Salehi, M. Kubicki, and A. Khaleghian, “New mononuclear copper(II) complexes from  $\beta$  -diketone and  $\beta$  -keto ester *N* -donor heterocyclic ligands: Structure, bioactivity and molecular simulation studies”, *J. Coord. Chem.*, 8972 (2018) 1–23.

[38] M. Shamsi, Sh. Yadav, F. Arjmand, “Synthesis and characterization of new transition metal {Cu(II), Ni(II) and Co(II)} L– phenylalanine–DACH conjugate complexes: In vitro DNA binding, cleavage and molecular docking studies”, *J. Photochem. Photobiol.*, 5(2014) 1-11.

[39] P. Yang, M. Guo, “Interaction of some non-Platinummetal anticancer complexes with nucleotides and DNA and the two-pole complementary principle (TPCP) arising therefrom”, *Metal-Based Drugs.* 5 (1998) 41–58.

[40] X.L. Wang, K. Zheng, L.Y. Wang, Y.T. Li, Zh.Y. Wu, C.W. Yan, “Synthesis and structure of a new ternary monocopper(II) complex containing mixed ligands of 2,2'-diamino-4,4'-bithiazole and picrate: in vitro anticancer activity, molecular docking and reactivity towards DNA”, *Appl. Organomet. Chem.* 30 (2016) 730-739.

[41] T. Daniel, Fisher, M. M. Appenheimer, Sh. S. Evans, “The two faces of IL-6 in the tumor microenvironment” *Seminars in Immun.*, 26 (2014) 38–47.

[42] V. S. Jones, R. Y. Huang, L. P. Chen, Zh. Sh. Chen, L. Fu, R. P. Huang, “Cytokines in cancer drug resistance: Cues to new therapeutic strategies” *BBA - Reviews on Cancer.*, 1865 (2016) 255-265.

[43] N. Kumari, B. S. Dwarakanath, A. Das, A. N. Bhatt, “Role of interleukin-6 in cancer progression and therapeutic resistance,” *Tumor Biol.*, 37 (2016) 11553–11572.

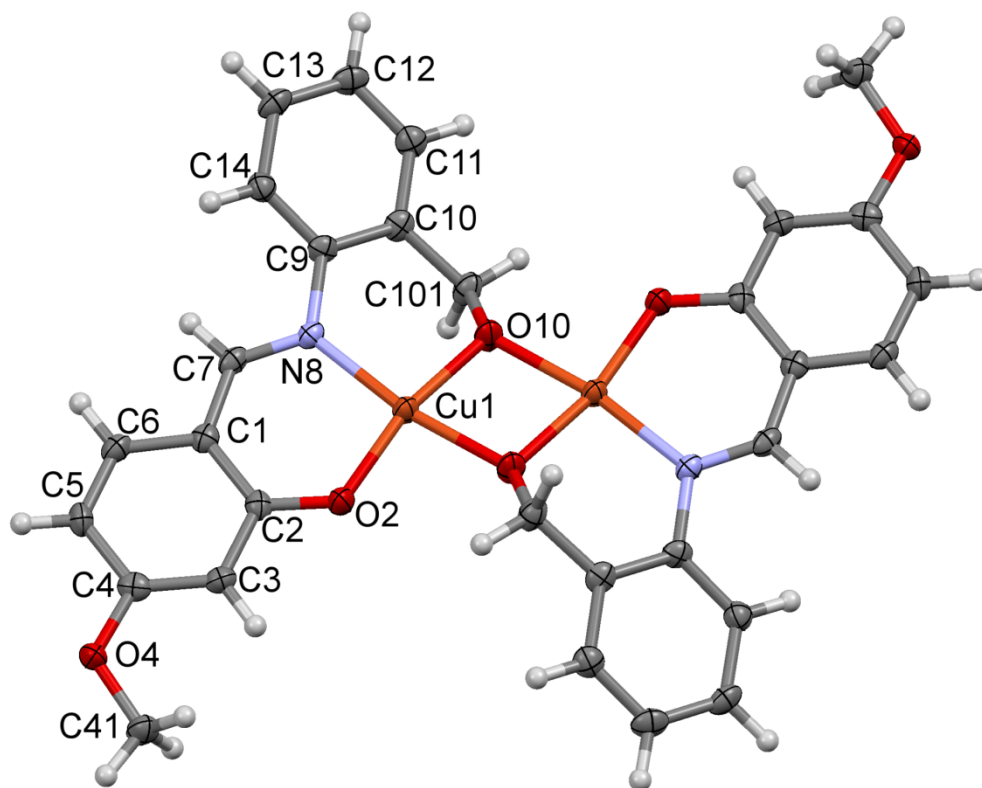


**Fig.1.** Perspective view of the complex 1; ellipsoids are drawn at the 70% probability level, hydrogen atoms are shown as spheres of arbitrary radii. Non-labelled atoms are related to the labelled ones by symmetry operation  $1-x, 2-y, 1-z$ .

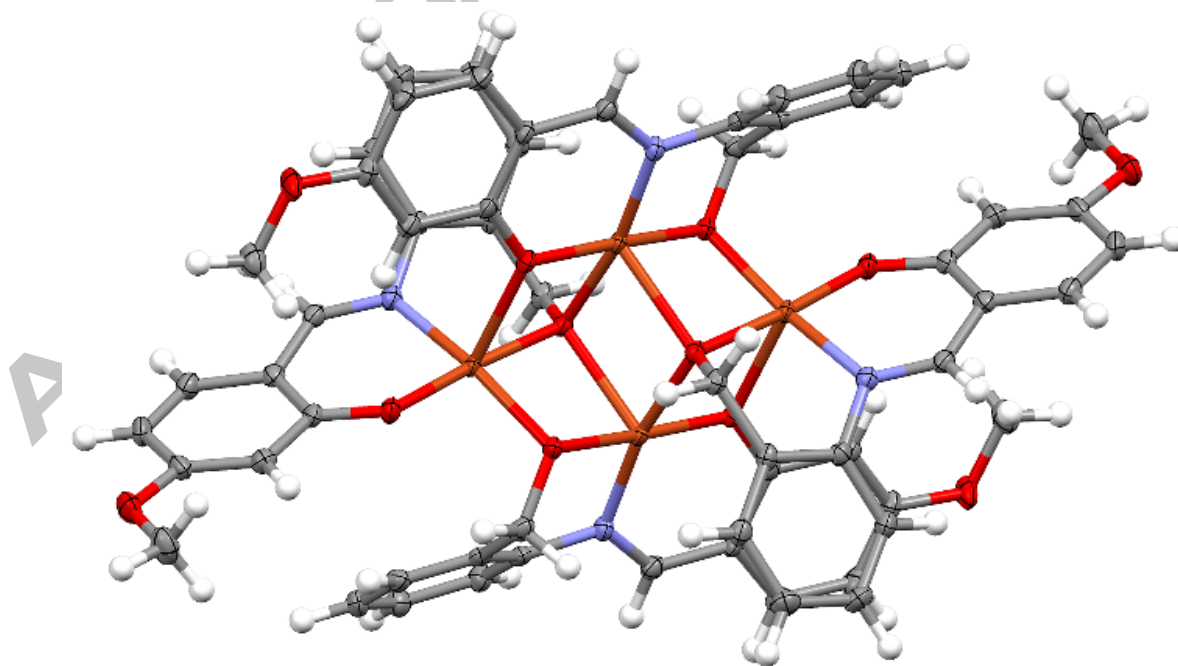


**Fig.2.** Perspective view of the complex **2**; ellipsoids are drawn at the 30% probability level; hydrogen atoms are shown as spheres of arbitrary radii.

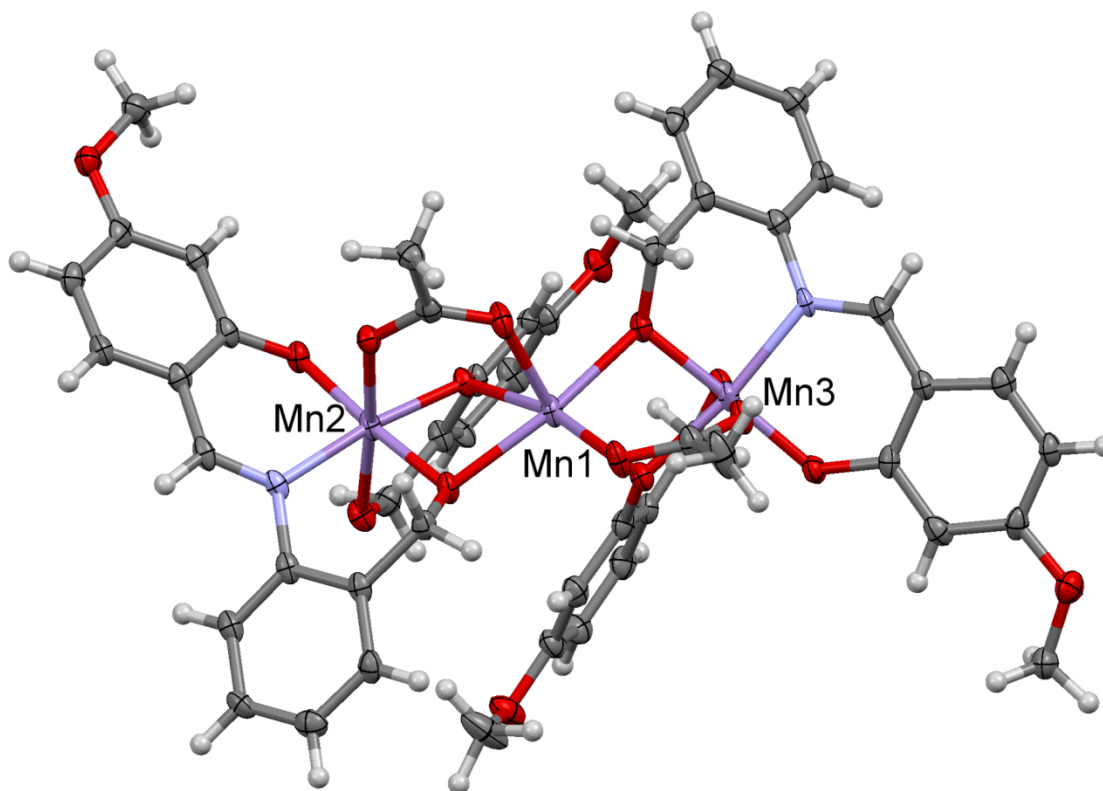


**Fig.3.** Perspective view of the complex **3**; ellipsoids are drawn at the 30% probability level; hydrogen atoms are shown as spheres of arbitrary radii.

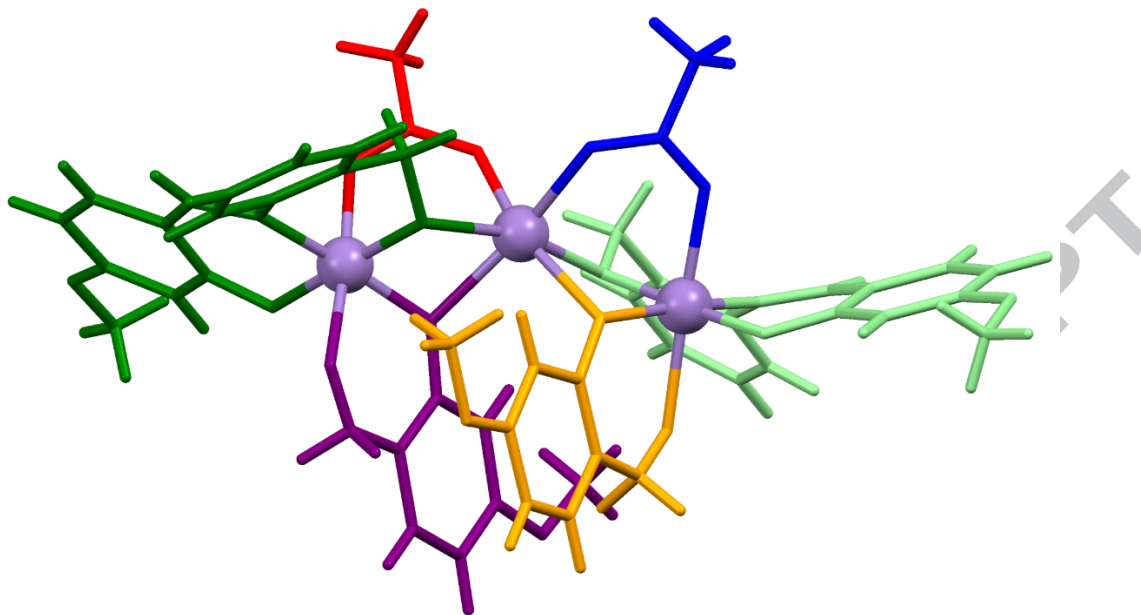


**Fig. 4.** Coordination of Mn cations; L<sup>1</sup> molecules are green, L<sup>2</sup> – orange and purple, acetates – blue and red.

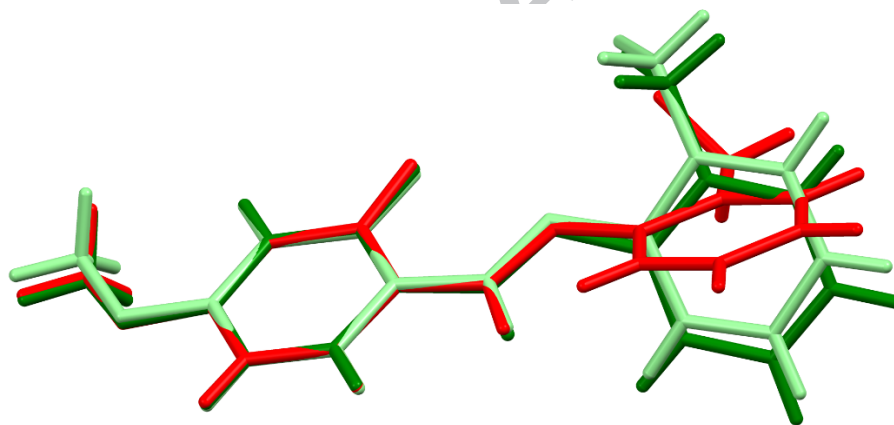


**Fig. 5.** Comparison of the L<sup>1</sup> conformations (red: **1**, green: two molecules in **3**); the phenyl A rings are fitted one onto another.

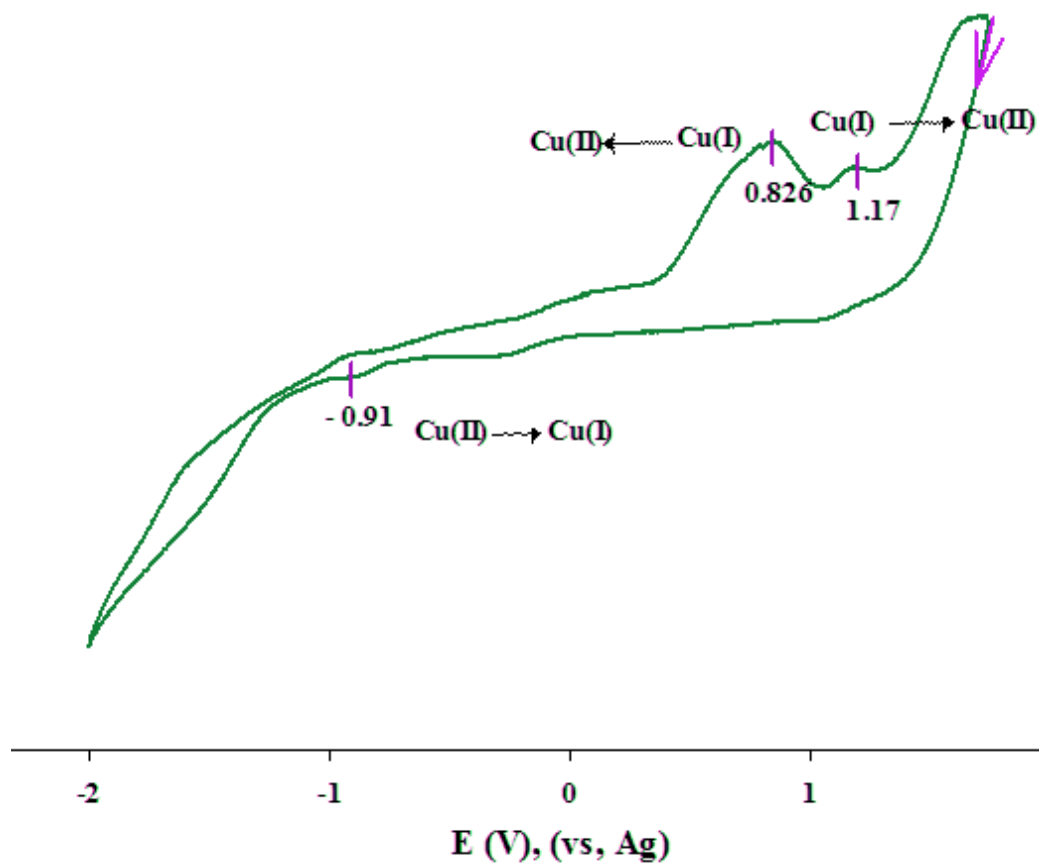


**Fig. 6.** Cyclic voltammogram of complex **1** ( $1 \times 10^{-3}$  mol/L / THF, 0.1 M tetrabutylammonium hexafluorophosphate (TBAH) at 100 mV/s).

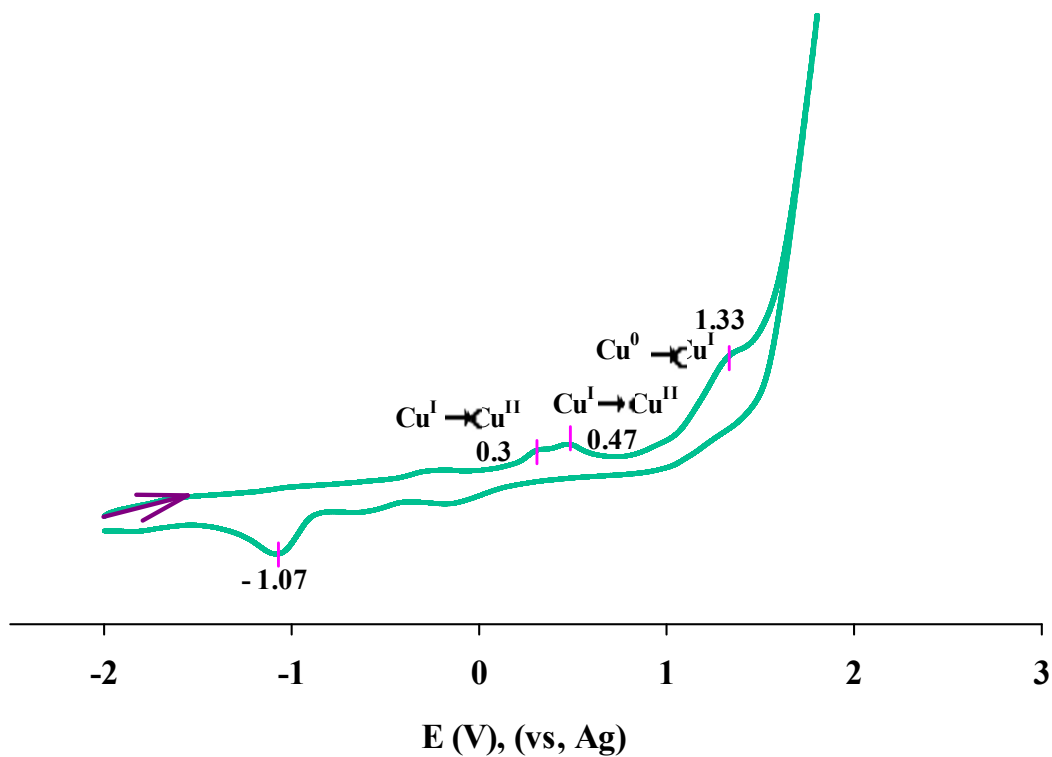


**Fig. 7.** Cyclic voltammogram of complex **2** ( $1 \times 10^{-3}$  mol/L / THF, 0.1 M tetrabutylammonium hexafluorophosphate (TBAH) at 100 mV/s).

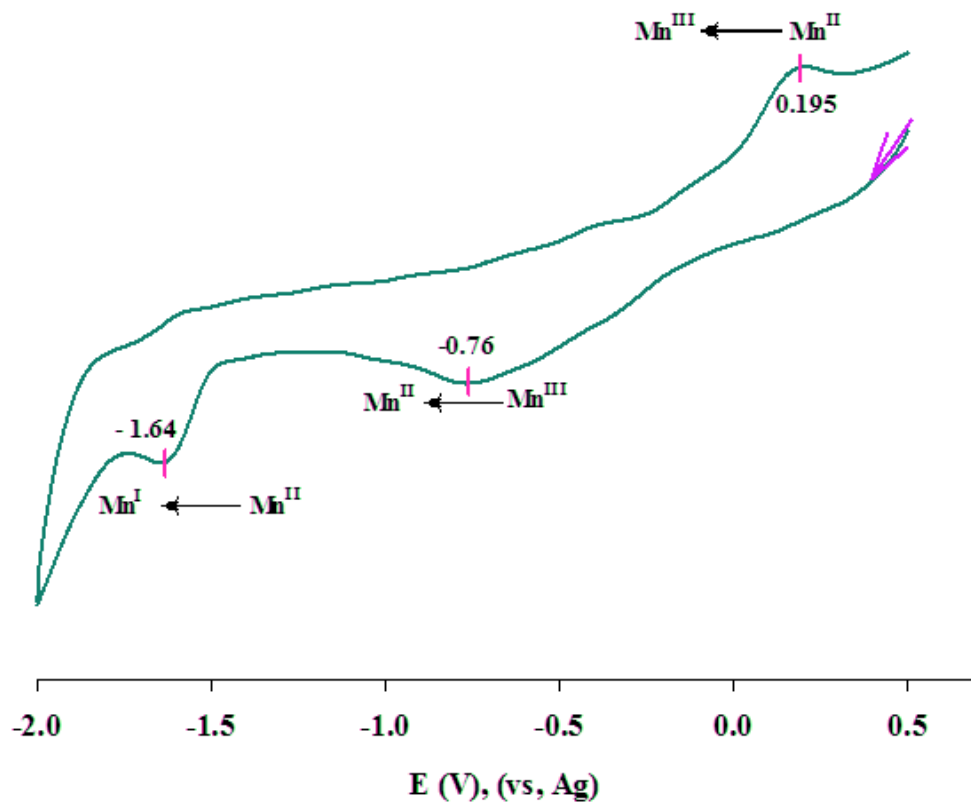
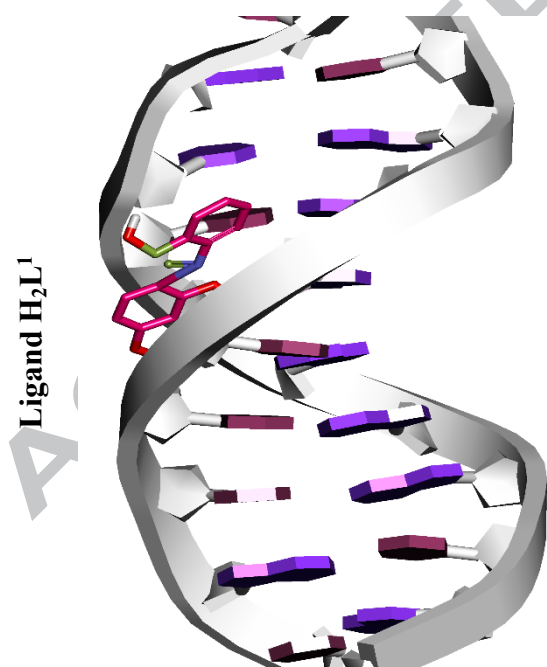
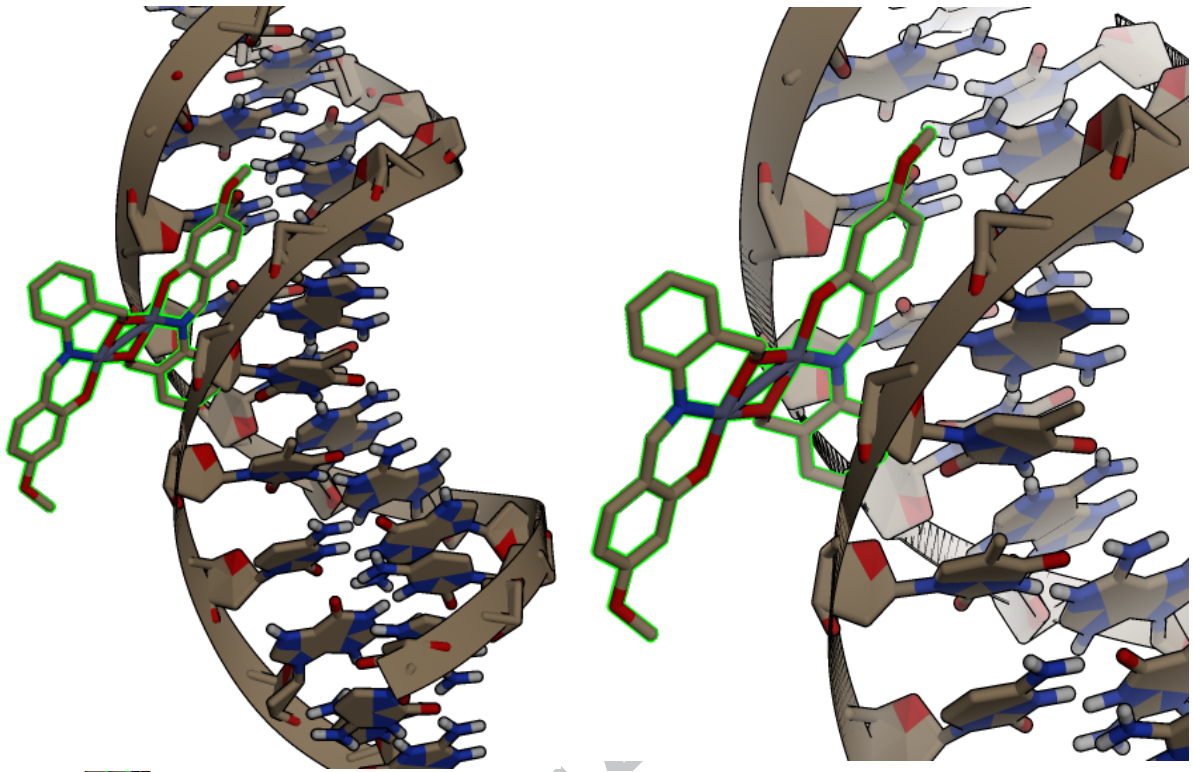


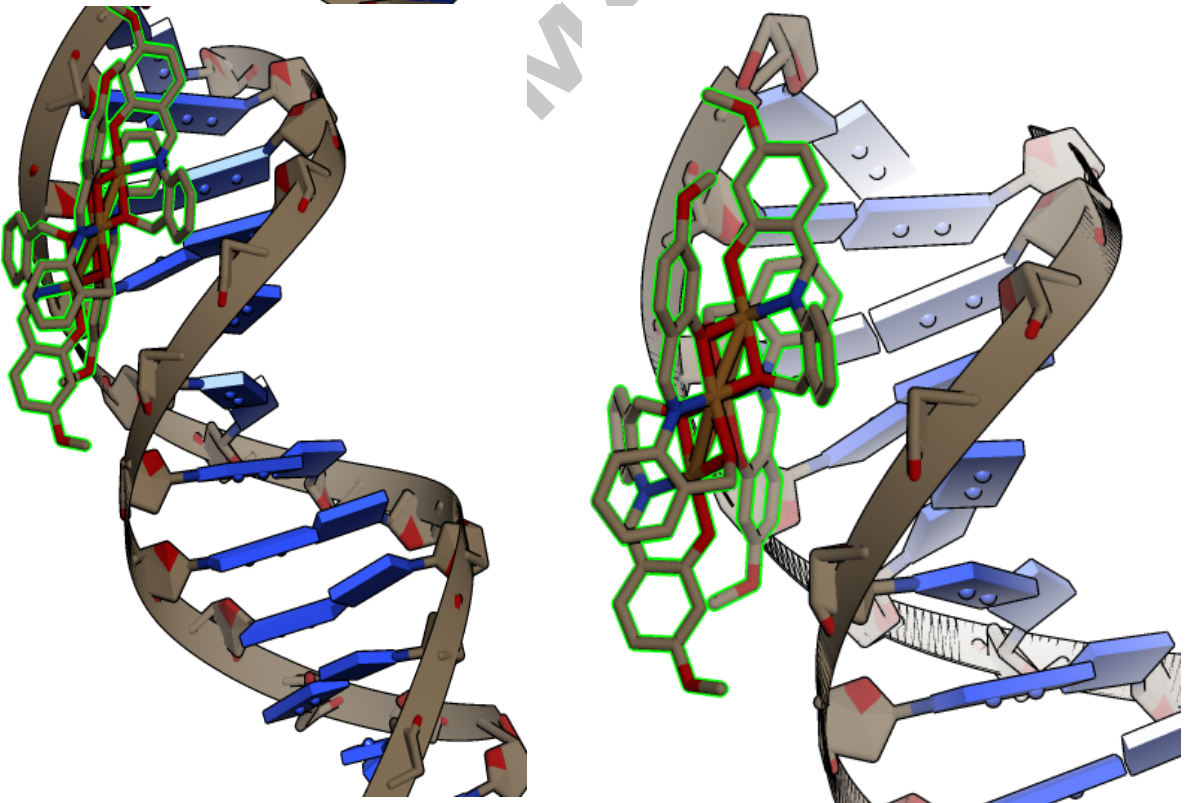
**Fig. 8.** Cyclic voltammogram of complex **3** ( $1 \times 10^{-3}$  mol/L / THF, 0.1 M tetrabutylammonium hexafluorophosphate (TBAH) at 100 mV/s).



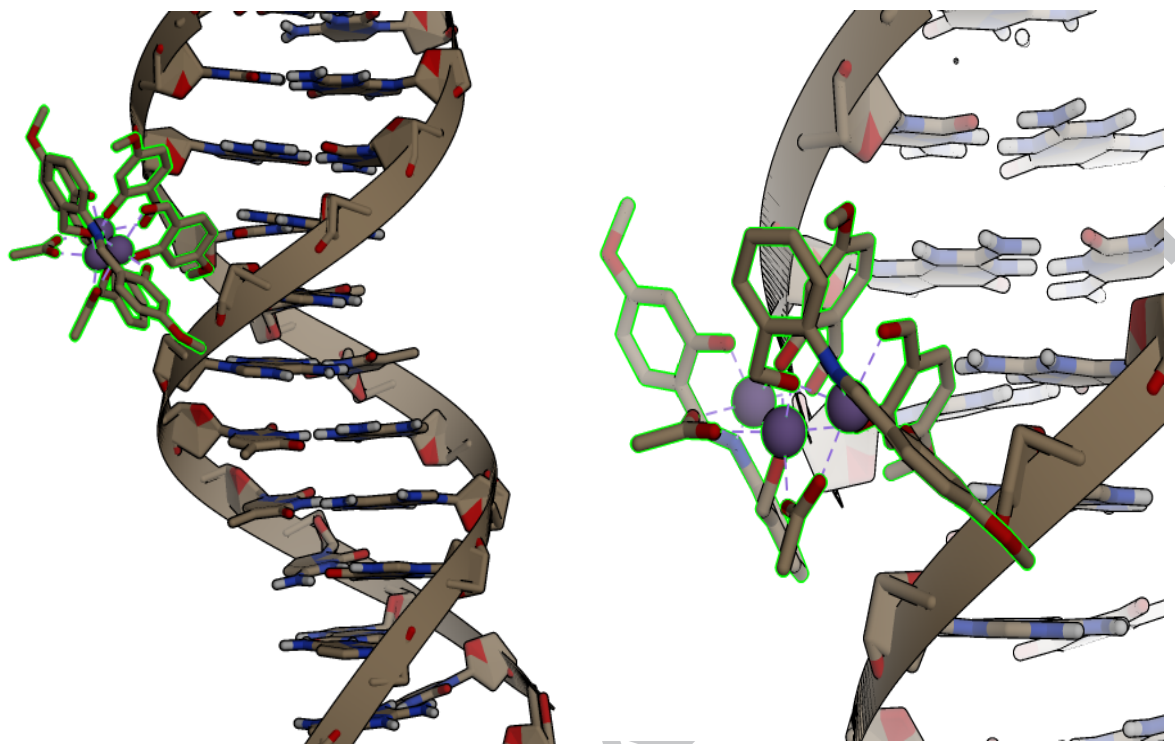
Complex 1



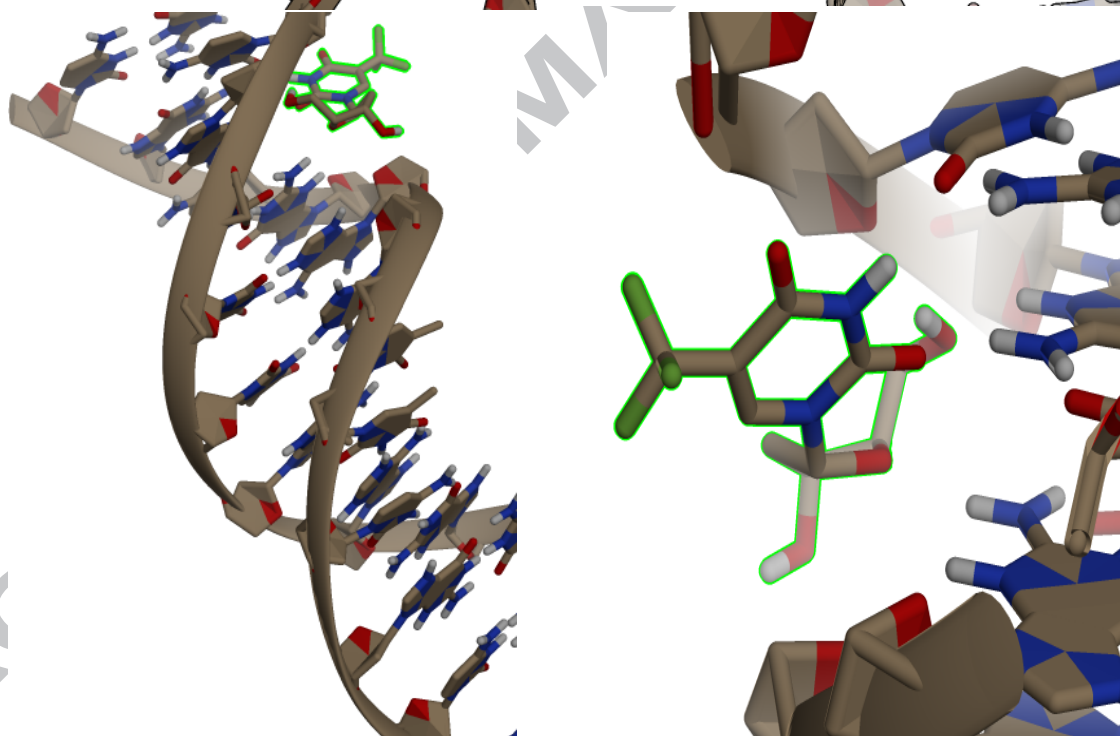
Complex 2

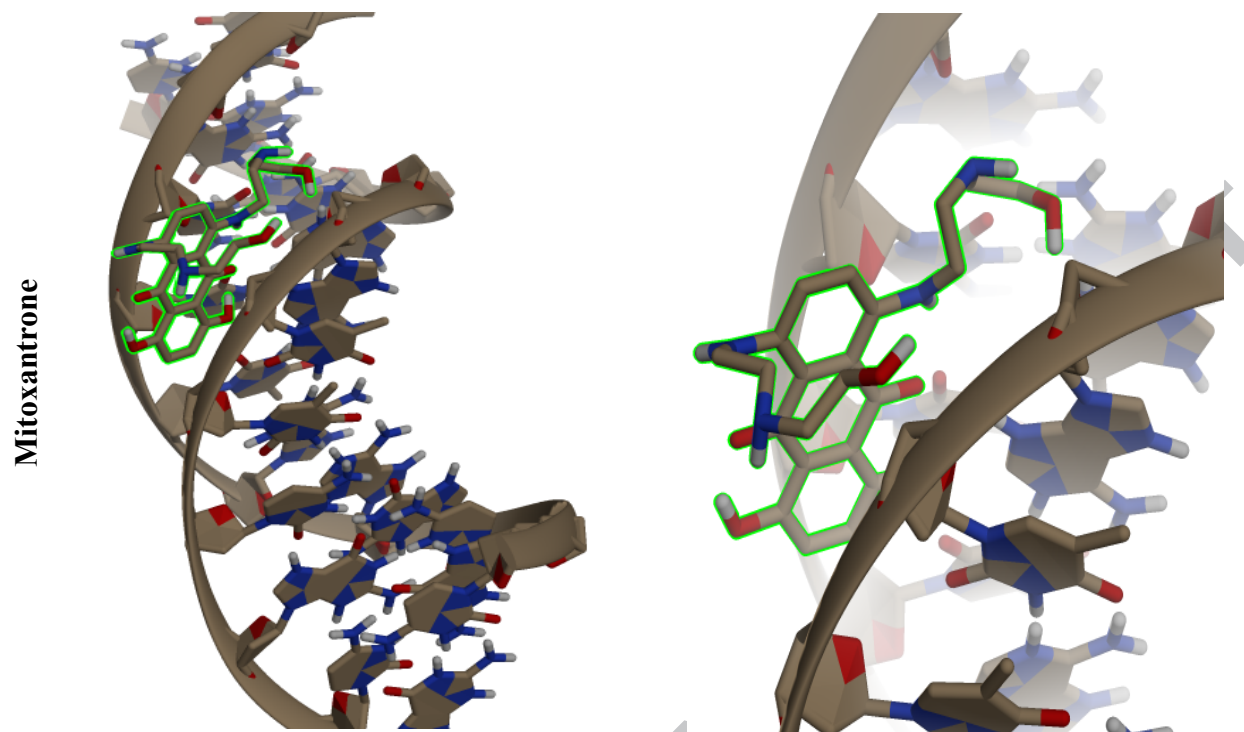


Complex 3

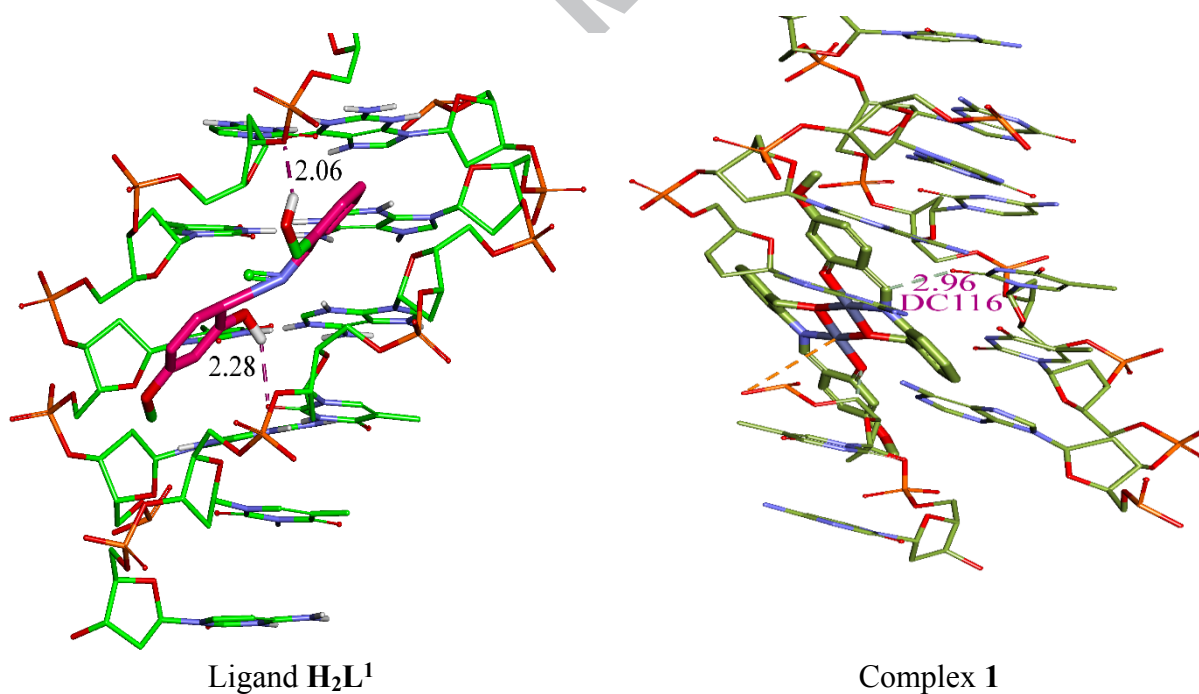


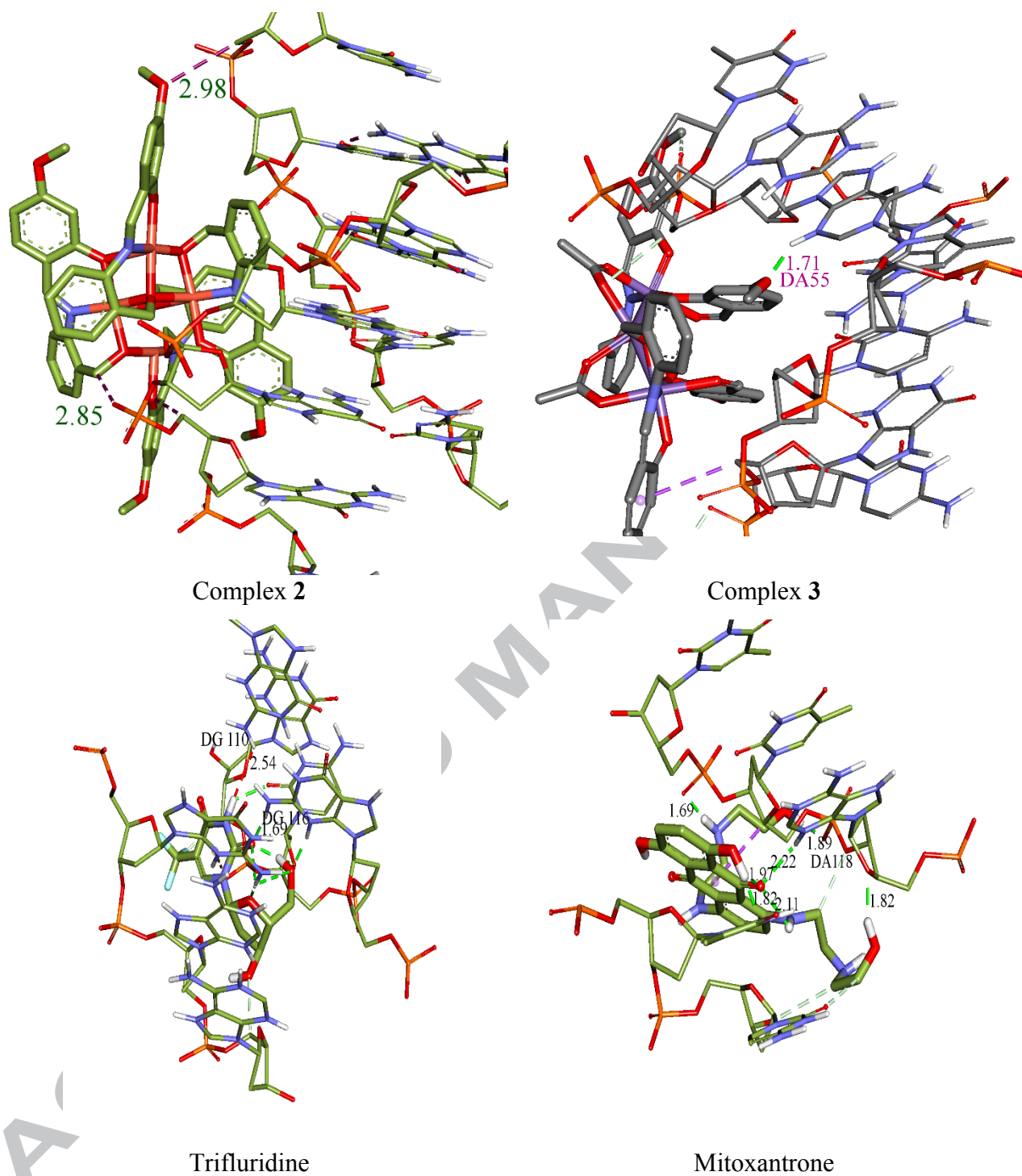
Trifluridine



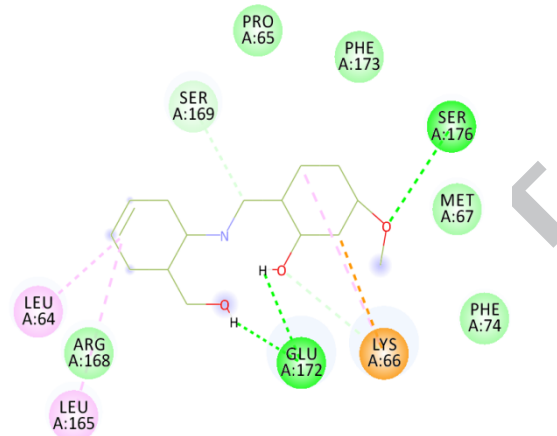
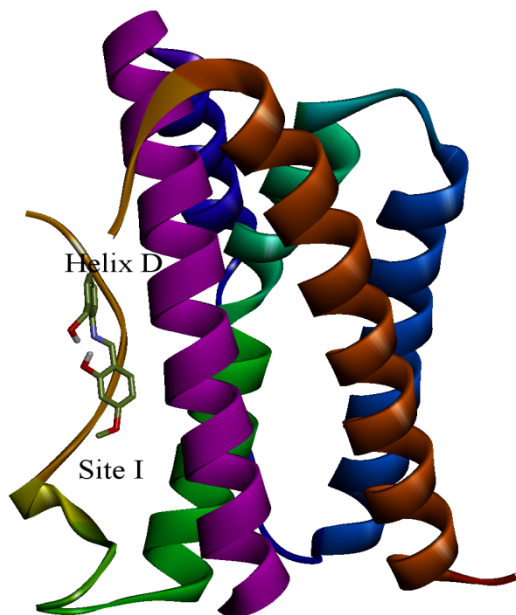


**Fig. 9.** Docking conformation of the ligand, complexes **1**, **2**, **3** and anti-cancer drugs to DNA (Trifluridine and Mitoxantrone).





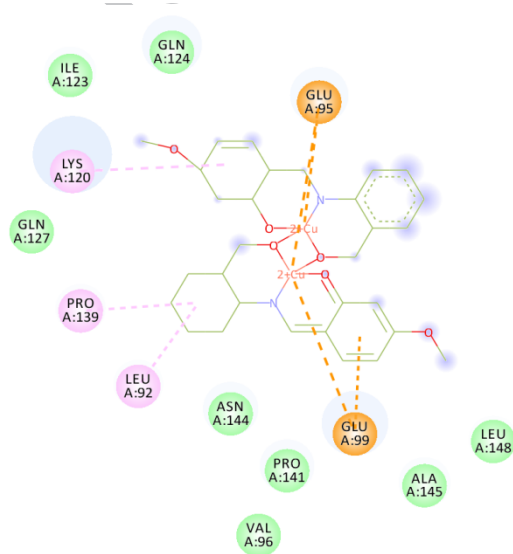
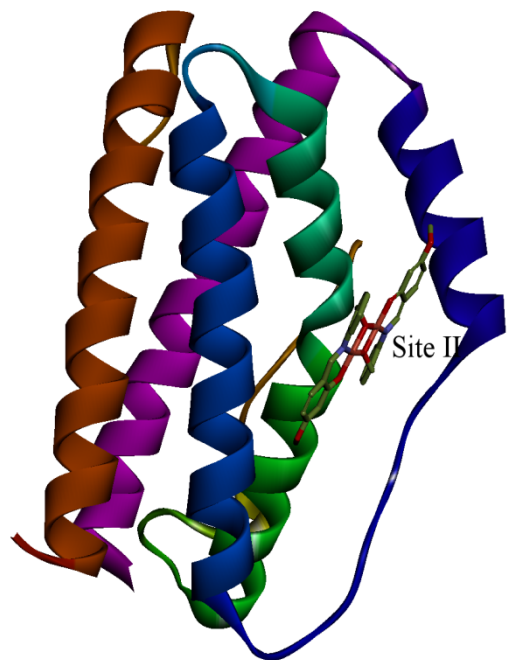
**Fig. 10.** Hydrogen bonding interactions of ligand, complexes 1, 2, 3 and anti-cancer drugs to DNA (Trifluridine and Mitoxantrone).

Ligand H<sub>2</sub>L<sup>1</sup>

## Interactions

- van der Waals
- Attractive Charge
- Conventional Hydrogen Bond
- Carbon Hydrogen Bond
- Alkyl

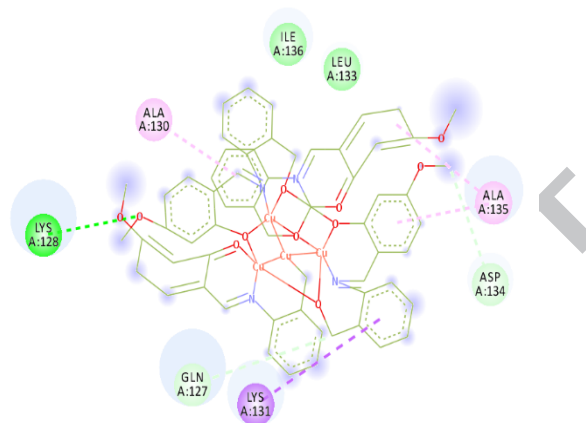
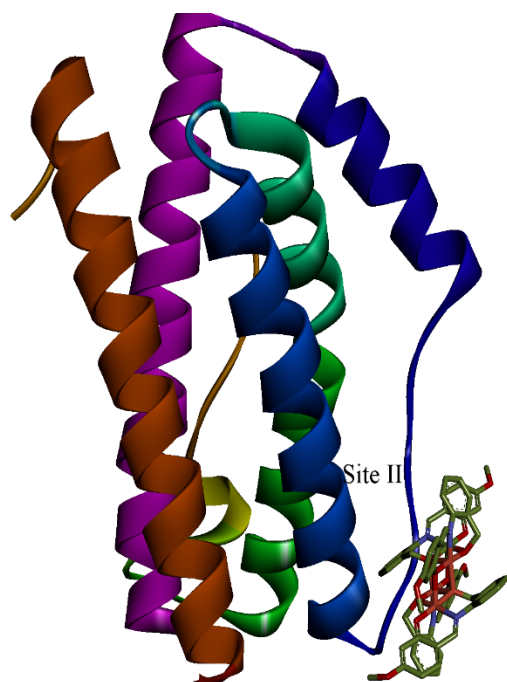
Complex 1



## Interactions

- van der Waals
- Attractive Charge
- Pi-Anion
- Alkyl

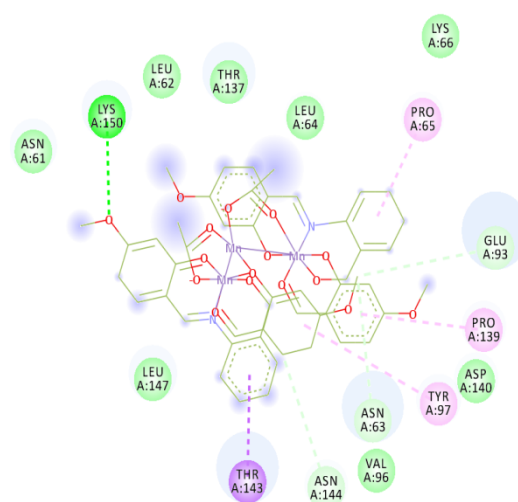
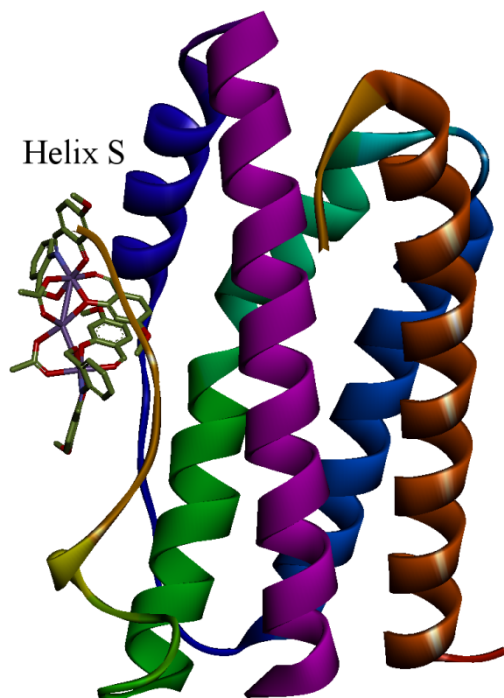
Complex 2



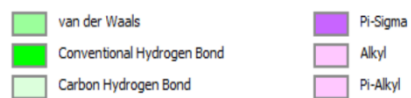
## Interactions



Complex 3



## Interactions



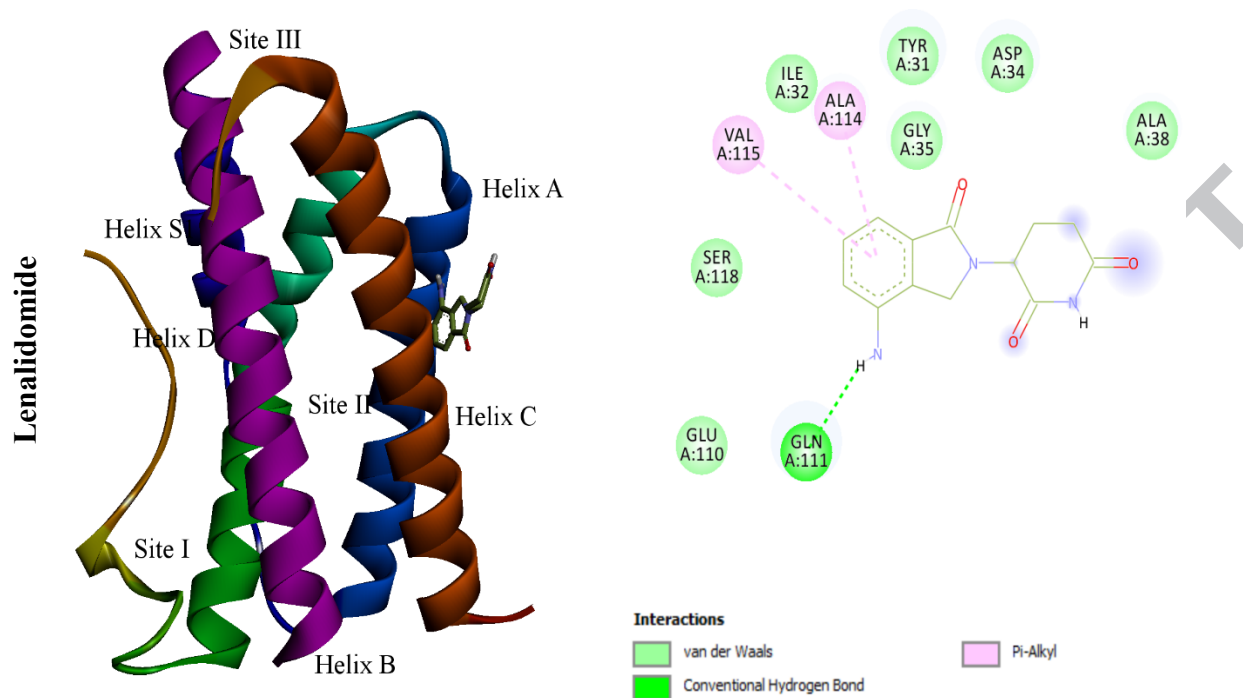


**Fig. 11.** Docking conformation of the ligand, complexes **1**, **2**, **3** and Lenalidomide with Interlukin-6.

**Table 1.** Crystal data, data collection and structure refinement.

Compound	<b>1</b>	<b>2</b>	<b>3</b>
Formula	$C_{30}H_{26}Cu_2N_2O_6$	$C_{60}H_{52}Cu_4N_4O_{12} \cdot (C_3H_7NO)$	$C_{50}H_{46}Mn_3N_2O_{16} \cdot C_2H_5OH$
Formula weight	637.61	1421.40	1141.77
Crystal system	monoclinic	Triclinic	monoclinic
Space group	$P2_1/n$	$P\bar{1}$	$P2_1/n$
$a$ (Å)	13.1899(5)	11.4839(8)	9.7436(7)
$b$ (Å)	4.7998(2)	12.4868(8)	24.8116(13)
$c$ (Å)	19.3964(7)	12.6384(7)	20.9121(12)
$\alpha$ (°)	90	72.073(6)	90
$\beta$ (°)	97.738(3)	66.176(6)	100.120(7)
$\gamma$ (°)	90	72.321(6)	90
$V$ (Å <sup>3</sup> )	1216.78(8)	1543.54(19)	4976.9(5)

$Z$	2	1	4
$D_x(\text{g cm}^{-3})$	1.740	1.529	1.524
$F(000)$	652	732	2356
$\mu(\text{mm}^{-1})$	3.348	1.431	0.826
$\Theta$ range ( $^\circ$ )	3.35 - 27.0	3.25 - 27.0	2.99 - 25.0
Reflections:			
Collected	12289	6228	45221
unique ( $R_{\text{int}}$ )	2509 (0.049)	754 (0.026)	8763 (0.116)
with $I > 2\sigma(I)$	2188	0.0466	5588
$R(F)$ [ $I > 2\sigma(I)$ ]	0.035	0.1223	0.074
$wR(F^2)$ [ $I > 2\sigma(I)$ ]	0.080	0.0577	0.171
$R(F)$ [all data]	0.043	0.1310	0.120
$wR(F^2)$ [all data]	0.086	1.062	0.193

**Table 2.** Selected geometrical parameters ( $\text{\AA}$ ,  $^\circ$ ) with s.u.'s in parentheses. A, B, C and D are the mean planes of planar fragments: p-methoxyphenyl ring (A), C-C=N -C chain (B) and phenyl ring (C). Symmetry code  $i$  1-x,2-y,1-z.

1		2		3					
Cu1-O2	1.8852(19)	Cu1-O17A	1.916(2)	Cu2-O17A	2.283(2)	Mn1-O1F	2.124(4)	Mn2-N8B	2.029(4)
Cu1-O10	1.901(2)	Cu1-O8A	1.929(2)	Cu2-O8A	1.973(2)	Mn1-O2E	2.150(4)	Mn2-O2F	2.161(4)
Cu1-O10 <sup>i</sup>	1.9467(18)	Cu1-N9A	1.986(3)	Cu2-N9B	1.985(3)	Mn1-O10B	2.150(4)	Mn2-O2C	2.214(4)
Cu1-N8	1.973(2)	Cu1-O8B	2.031(2)	Cu2-O8B	1.971(2)	Mn1-O10A	2.153(4)	Mn3-O10A	1.882(4)
		Cu1-O8B <sup>i</sup>	2.234(2)	Cu2-O17B <sup>i</sup>	1.909(2)	Mn1-O1D	2.245(4)	Mn3-O2A	1.889(4)
						Mn1-O1C	2.268(4)	Mn3-O1D	1.967(4)
						Mn2-O2B	1.890(4)	Mn3-N8A	2.018(4)
						Mn2-O10B	1.891(4)	Mn3-O1E	2.169(4)
						Mn2-O1C	1.952(4)	Mn3-O2D	2.226(4)
Cu1...Cu1 <sup>i</sup>	3.0187(7)	Cu1...Cu2 <sup>i</sup>	3.0449(6)			Mn1...Mn2	3.1053(11)	Mn1...Mn3	3.1245(11)
				Cu1	Cu2		Mn1	Mn2	Mn3
N8-Cu1-	170.20(9)		174.39(9)	175.65(9)		3 largest	167.85(14)	176.16(16)	176.93(17)

O10 <sup>i</sup>	167.87(8)	169.13(10)	166.40(10)	angles	163.95(14)	175.19(14)	175.35(14)
O2-Cu1-O10		110.63(10)	103.71(9)		160.07(14)	171.71(18)	170.29(17)
		Ligand A	Ligand B		Ligand A	Ligand B	
A/B	6.15(13)	13.06(12)	22.04(15)		21.7(3)	16.7(5)	
B/C	18.33(19)	39.62(15)	42.38(18)		41.5(4)	37.6(4)	
A/C	23.17(13)	50.57(12)	58.09(13)		57.82(18)	50.69(19)	

**Table 3.** DNA docking results of the compounds ligand, **1**, **2**, **3** and anti-cancer drugs to DNA (Unit:kcal/mol)

	Ligand	1	2	3	Mitoxantron	Trifluridine
Estimated Free Energy of Binding <sup>a</sup> (kcal/mol )	-7.56	-7.74	-6.45	-9.87	-9.09	-5.88
Final Intermolecular Energy (kcal/mol )	-9.21	-8.84	-7.55	-10.41	-13.87	-7.33
vdW + Hbond + desolv Energy (kcal/mol )	-9.13	-8.56	-7.56	-10.41	-10.22	-6.71
Electrostatic Energy (kcal/mol )	-0.08	0.28	-0.02	0.05	-3.64	-0.67
Final Total Internal Energy (kcal/mol )	-0.65	0.94	-0.80	0.12	-3.93	-0.84
Torsional Free Energy (kcal/mol)	1.65	+1.10	1.1	0.55	4.77	1.49
Unbound System's Energy (kcal/mol )	-0.65	0.94	-0.80	0.12	-3.93	-0.84

$$a)\Delta G_{\text{binding}} = \Delta G_{\text{vdW+hb+desolv}} + \Delta G_{\text{elec}} + \Delta G_{\text{total}} + \Delta G_{\text{tor}} - \Delta G_{\text{unb}}$$

**Table 4.** Docking results of the compounds ligand, **1**, **2**, **3** and Lenalidomide (Interlukin-6 inhibitor) (Unit:kcal/mol) with Interlukin-6 (1alu).

	Ligand	1	2	3	Lenalidomide,
Estimated Free Energy of Binding <sup>a</sup> (kcal/mol )	-5.71	-7.66	-7.72	-7.70	-6.34
Final Intermolecular Energy (kcal/mol )	-7.50	-8.26	-8.91	-8.89	-6.94
vdW + Hbond + desolv Energy (kcal/mol )	-7.08	-7.96	-8.54	-8.84	-6.93
Electrostatic Energy (kcal/mol )	-0.42	0.30	-0.38	0.05	-0.01

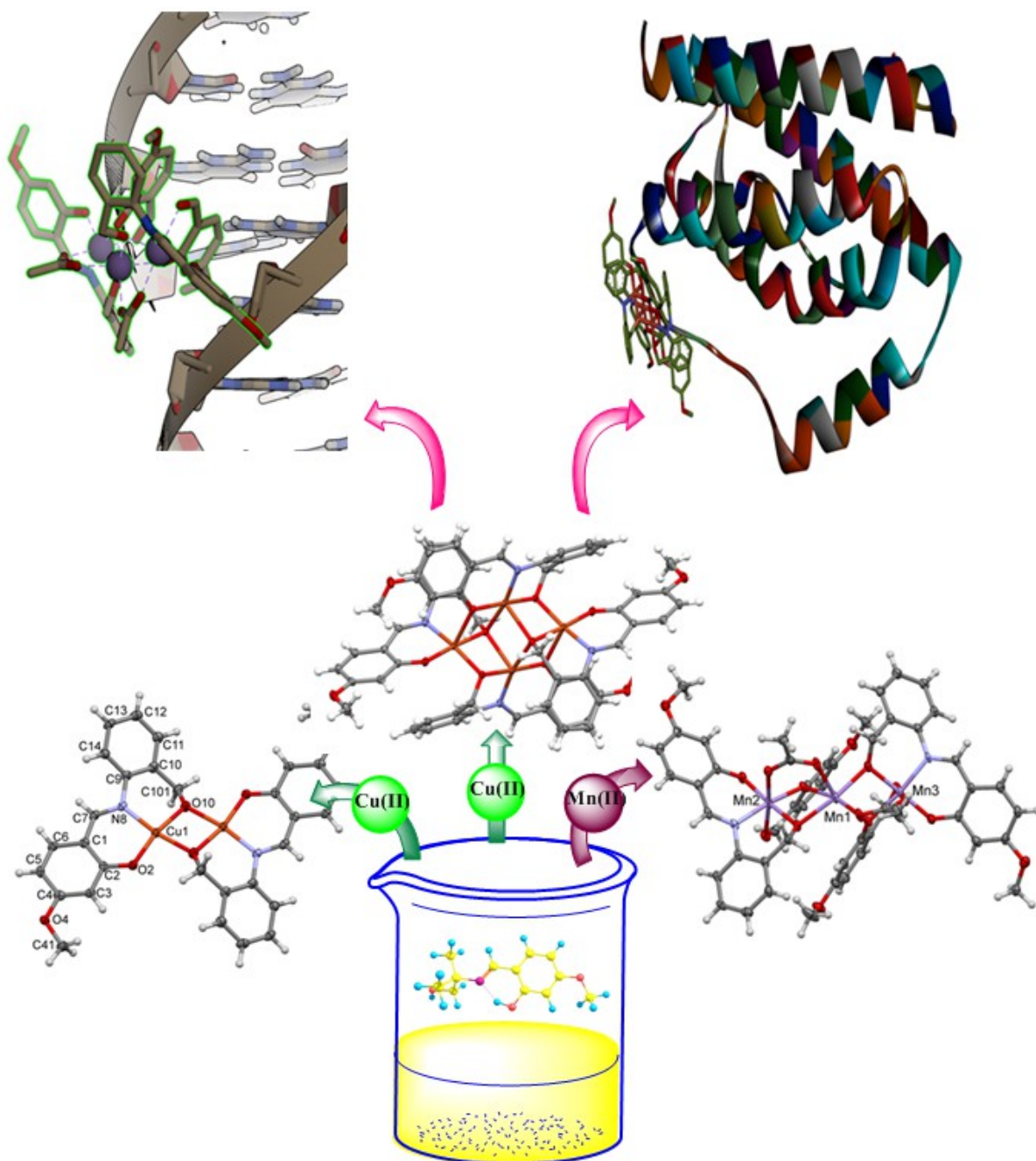
Final Total Internal Energy (kcal/mol )	-2.60	0.13	-0.60	0.79	-0.07
Torsional Free Energy (kcal/mol)	1.79	0.60	1.19	1.19	0.6
Unbound System's Energy (kcal/mol )	-2.60	0.13	-0.60	0.79	-0.07

---

$$a)\Delta G_{\text{binding}} = \Delta G_{\text{vdW+hb+desolv}} + \Delta G_{\text{elec}} + \Delta G_{\text{total}} + \Delta G_{\text{tor}} - \Delta G_{\text{unb}}$$

### Graphical abstract

Three new poly-nuclear complexes Cu(II) and Mn(II) were synthesized and characterized by elemental analysis, FT-IR, UV/Vis and electrochemical behavior. Also, molecular structures of complexes were determined by X-ray crystallography. The docking study provided useful structural information for inhibition studies.



### Highlight

- Metal complexes of the Schiff base were synthesized.
- The crystal structures of the complexes were determined by X-ray crystallography.
- Cyclic voltammograms of all complexes were studied.
- The molecular docking studies of synthesized complexes were carried out.

ACCEPTED MANUSCRIPT